TÉCNICO LISBOA

The impact of low salinity on oil recovery from a carbonate reservoir

Diana Sofia Patrício da Silva

Thesis to obtain the Master of Science Degree in:

Petroleum Engineering

Supervisors: Professor Doctor Maria João Correia Colunas Pereira
Engineer María Rosario Rodriguez Pardo

Examination Committee

Chairperson: Professor Doctor Maria Teresa da Cruz Carvalho
Supervisors: Professor Doctor Maria João Correia Colunas Pereira
Members of the Committee: Engineer Nicolas Blin

November 2015

Abstract

Carbonates reservoirs have a high presence around the world. However their characteristics are challenging, which has led to the necessity of studying this type of reservoirs and its oil production through different methods. The work developed aims to study the impact of salinity and anions on the wettability and oil recovery in a carbonate reservoir rock, in Abu Dhabi.

It is already comproved that injecting brine with low salinity increases the oil recovery and some of the ions present, like sulphate, calcium and magnesium are the responsible. When the concentrations of non-active ions are reduced, these active ions have easier access to the carbonate surface, improving the oil recovery, through wettability alteration.

The work consists in an EOR core flooding experiment with the purpose of reproducing the reservoir conditions. To achieve this goal, four limestone outcrops were saturated with synthetic water, saturated with oil until reach the irreducible water saturation, aged at the reservoir temperature, injected with oil to measure the oil permeability and finally aged again to make the fluids adhere to the rock and restore wettability.

After the reached initial reservoir conditions, water with different salinity was injected, to analyse the effect of this method in the oil recovery.

Keywords: Carbonates, Low Salinity, Wettability, Enhanced Oil Recovery

Resumo

A presença de Reservatórios carbonatos no mundo é elevada, no entanto as suas características são desafiadoras, o que conduziu à necessidade de estudar este tipo de reservatório e a sua produção de petróleo através de diferentes métodos. O trabalho desenvolvido tem como objetivo estudar o impacto da injeção de água com baixa salinidade e de alguns aniões na molhabilidade e recuperação de petróleo de um reservatório carbonatado, em Abu Dhabi.

Está comprovado que injetar salmoura com baixa salinidade aumenta a recuperação de petróleo, sendo que alguns iões presentes, como sulfato, cálcio e magnésio, iões ativos, contribuem para este aumento. Quando a concentração de iões não ativos é reduzida, os iões ativos têm mais fácil acesso à superfície da rocha, aumentando a recuperação de petróleo, através da alteração de molhabilidade.

O trabalho desenvolvido consiste em diversos trabalhos experimentais de coreflooding (injeções num provete) nos quais são reproduzidas as condições de reservatório, deste modo, quatro provetes de *limestone* foram saturados com salmoura sintética, com as mesmas características da água existente na formação, saturados com petróleo até atingir a saturação de água irredutível, envelhecidos à temperatura de reservatório, onde foi medida a permeabilidade da rocha ao petróleo através da injeção de petróleo e finalmente deixados à temperatura reservatório, envelhecendo, de modo a que os fluidos presentes adiram à rocha e a molhabilidade seja restaurada.

Depois do provete ser sujeito a todas as condições iniciais de reservatório, foi injetada água com diferente salinidade, e analisado o efeito deste método na recuperação de petróleo.

Keywords: Carbonato, Baixa salinidade, Molhabilidade, Recuperação melhorada de petróleo

Acknowledgements

This thesis would not have been possible without the CEPSA research center. It was an honour for me to work in this place. I am grateful to all the personnel from CEPSA that received me so well, especially to Exploration and Production department. I would like to thank Rosario Rodriguez, Nicolas Blin, Jesus Montes, Pedro Romero, Carlos Prieto, Flor Garcia, Asier Panadero, Juan José Suñer and José María Castro for all their help, support, trust and time invested in me and all the interns that shared the laboratory with me.

I also would like to show my gratitude to my school, Instituto Superior Técnico, to all my professors and colleagues during this course, especially to my advisor Maria João Pereira and all my master colleagues.

I owe my deepest gratitude to my family and friends, especially to my parents and brother, that always helped me in my choices. Additively to all my friends that has became part of my life and showed me them support, both in Spain and Portugal, and always support me.

It is a pleasure to thank those who made this thesis possible, and it was a great pleasure realize this thesis.

To all that made it a little bit more possible, sincerely thank you.

Contents

List of Tables

List of Figures

List of Acronyms

$(CaCl_2.2H_2O)$ Calcium chloride di-hydrate

(Ca^{2+}) Calcium

(KCl) Potassium chloride

$(MgCl_2.6H_2O)$ Magnesium chloride hexahydrate

(Mg^{2+}) Magnesium

$(NaCl)$ Sodium chloride

$(NaHCO_3)$ Sodium bicarbonate

(Na_2SO_4) Sodium sulfate

(SO_4^{2-}) Sulphate

ADNOC Abu Dhabi National Oil Company

BF Back/Reverse flow

BPR Back Pressure Regulator

CC Coreflooding carbonate

CIC CEPSA investigation center

DP Differential Pressure

EOR Enhanced oil recovery

EP Exploration and Production

FB Formation Brine

IFT Interfacial tension

Kro Relative oil permeability

NA Not Available

NF Normal flow

OOIP Original oil in place

PV Pore Volume

Pc Capillary pressure

SSW 1/10 Synthetic Seawater diluted 10 times

SSW 1/25 Synthetic Seawater diluted 25 times

SSW mod Synthetic Seawater modified

SSW Synthetic Seawater

So Oil saturation

Swi Irreducible water saturation

Sw Water saturation

TDS Total Dissolved Solids

UAE United Arab Emirates

Chapter 1

Introduction

The work developed took place at the Research center of CEPSA, in Exploration and Production (E&P) department. CEPSA, Compañía Española de Petróleos, S.A.U. is a Spanish multinational oil and gas Company. The Exploration and Production (E&P) department aims in their work to maximize the percentage of oil recovery in the fields, and to do that, the company is developing techniques for Enhanced Oil Recovery (EOR) applicable to current and future assets.

It is estimated that more than 60 percent of the world's oil and 40 percent of the world's gas reserves are held in carbonate reservoirs. More specifically, the Middle East is dominated by carbonate fields, with around 70 percent of oil and 90 percent of gas reserves held in these reservoirs.

Due to the high presence of carbonate reservoirs around the world, Fig. 1.1, is important to study the carbonate behaviour.

Its mineralogy is formed principally by calcite, dolomite and minor clay, but this type of rocks is quite complex because of its heterogeneity. Carbonates are characterized by different types of porosity and complex pore size distributions which result in wide range of permeability .

Besides, it is estimated that 80 - 90 percent of the world's carbonate reservoirs are preferentially oil-wet and they exhibit negative capillary pressure, which leads to low oil production. All these reasons make important to study carbonate reservoirs and their production.

The work developed aims to study the impact of salinity and anions on the wettability of a carbonate reservoir rock and oil recovery in an Abu Dhabi oil field. Literature data show that Ca^{2+}, Mg^{2+}, and SO_4^{2-}, present in brine, are active ions in the wettability alteration process to water-wet, due to the strong affinity of sulphate, it can be adsorbed on the carbonates surface and it reduces the positive charge density.

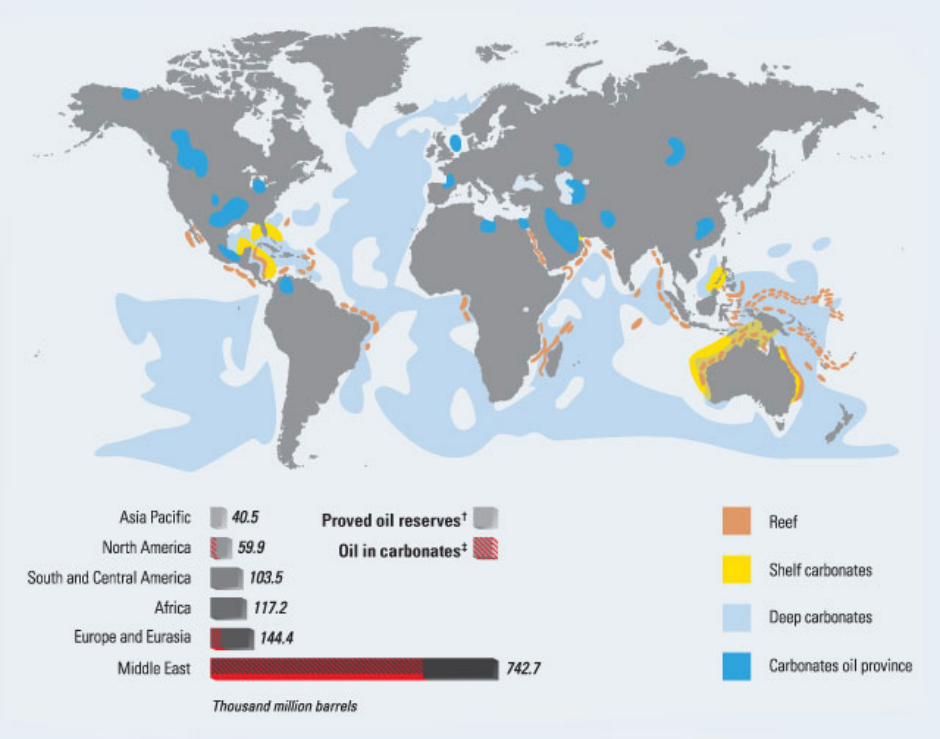

Figure 1.1: Distribution of oil from carbonate sources around the world. [1]

During this study EOR core flooding experiments were performed in four cores. In these experiments, it is important to reproduce, as much as possible the initial conditions of the rock, such as fluids saturation and wettability. Therefore, each core must be exposed during the right time to the various stages of the experiments.

Thus, the objectives of this work are to investigate the effect of salinity on the wettability of a carbonate reservoir rock, in order to analyse the productivity of carbonate rocks.

1.1 Outline

This document describes the research and work developed and it is organized as follows:

- **Chapter 2** presents the background important to the work developed.
- **Chapter 3** describes the material used in the experiment, such as cores, brines, oil and other equipment.
- **Chapter 4** presents the experimental methodology used in the cores preparation and in core flooding.

- **Chapter 5** describes the results of the experiment.
- **Chapter 6** summarizes the work developed and suggests further developments.
- **Appendix** section contains supplementary material.

Chapter 2

Literature Review

2.1 Carbonate Reservoirs

The presence of carbonate reservoirs around the world is very high and the greatest concentration of large oil fields in the world is in the Middle East. It is estimated that half or more of the world's petroleum is produced from this type of reservoirs, therefore it is important to study the carbonate behaviour.

Carbonates are difficult to characterize because they can have highly varying properties, like porosity, permeability and flow mechanisms, within small sections of the reservoir. Therefore it is necessary a focused approach to better understand the heterogeneous nature of the rock containing the fluids and the flow properties within the porous and often fractured formations. [9]

2.1.1 Sedimentary rocks

Sedimentary rocks are a type of rocks that are formed by sedimentation of materials, on or near the Earth's surface. The name sedimentation, describes processes that cause mineral and/or organic particles (detritus) to settle and accumulate or minerals to precipitate from a solution. Particles that form a sedimentary rock by accumulation are called sediments. Before being deposited, sediments were formed by weathering and erosion in a source area, and then transported to the place of deposition by water, wind, mass movements or glaciers. For the transition from sediments to sedimentary rocks, a long deposition time is needed, and geological processes like compaction and/or cementation are necessary.

Sedimentary rocks have some particular characteristics such as their sedimentary facies and texture. It usually feature banking, and other characteristic structures, like bedding. Analyzing each layer of a sedimentary rock it is possible to know the deposition conditions, such as source material (often

containing organisms, like mussels, brachiopods and others, being present in the sedimentary rock by their shells or ichnia) and the means of transport. [10]

There are three basic types of sedimentary rocks:

- **Clastic sedimentary rocks** such as breccia, conglomerate, sandstone and shale, that are formed from mechanical weathering debris;
- **Chemical sedimentary rocks** such as rock salt and some limestones, that are formed from the precipitation of dissolved materials in solution;
- **Organic sedimentary rocks** such as coal and some limestones which were formed from the accumulation of plant or animal debris.

2.1.2 Carbonates

Carbonates are sedimentary rocks mainly composed primarily of carbonate minerals. The two major types of carbonates are limestone, which is composed by mostly calcite or aragonite (different crystal forms of $CaCO_3$) and dolostone, which is predominantly composed by mineral dolomite $(CaMg(CO_3)_2)$. Therefore carbonate rocks are made of particles (composed by more than 50 percent of carbonate minerals) embedded in a cement.

Most carbonate rocks result from the accumulation of bioclasts created by organisms, many small lime (CaO) secreting animals, plants, and bacteria live in the shallow water. Their secretions and shells form many of the carbonate rocks. Thus, this type of rock is common in shallow marine environments and warm seas, i.e. in areas favourable to biological activity.

The economic importance of carbonate rocks is due to their rich organic content and good reservoir properties. [10, 11]

2.1.3 Limestone

Limestone is a sedimentary rock composed mainly of calcium carbonate $(CaCO_3)$, usually calcite and sometimes aragonite. Most limestones are formed organically from the accumulation of shell, coral, algal and fecal debris. They can also be formed chemically from the precipitation of calcium carbonate from lake or ocean water.

Clark is a particular type of limestone composed of accumulated deposits of skeletal or shell remains of microscopic animals. [10]

2.2 Oil Field details

The carbonate reservoir under study is located in Abu Dhabi, United Arab Emirates (UAE), Fig. 2.2.

Figure 2.2: Abu Dhabi Map. [2]

2.2.1 Oil field details

- **Company Name:** Abu Dhabi National Oil Company (ADNOC)
- **Country:** UAE
- **State:** Abu Dhabi
- **Reservoir Temperature (°C):** 120 °C
- **Reservoir Permeability (*mD*):** 10
- **Reservoir geology Type:** Carbonate
- **Formation geology Type:** Limestone
- **Operating Pressure (*psia*):** 2500-3000

2.2.2 Brine details

The brine composition is given in Table 2.1. The data represents the average concentration of 6 brine analyses from one well:

Composition	Brine from the oil field (*mg/l*)
Choride	114363.17
Sulphate	273.33
Carbonate	NL
Bicarbonate	368.00
Calcium	16666.67
Magnesium	1570.00
Iron	135.00
Sodium	52235.67

Table 2.1: Brine details

2.2.3 Oil details

Data from a well:

- **Crude oil API gravity:** 35.6° at 15.5 °C
- **Crude oil viscosity:** 1.07 *mPa.s* at 120 °C
- **Crude oil density:** 0.8292 *kg/l* at 37.8 °C

2.3 Oil Recovery

The process to extract oil from the reservoirs can be subdivided into three stages: primary, secondary, and tertiary recovery. Often, reservoir production operations are not performed in the specified order that tertiary process can be applied in secondary stage instead of waterflooding. Thus, the designation of Enhanced oil recovery (EOR) became more accepted, and the term tertiary recovery became obsolete.

Natural production depends on a reservoir's internal energy, and the oil rises due to the existence of an higher pressure in the rock pores than at the bottom of the well. All other recovery methods depend on the provision of additional energy to improve the recovery of the remaining oil in the reservoir.

2.3.1 Primary Recovery

During primary recovery, the natural pressure of the reservoir or gravity drive oil into the wellbore, and the artificial lift techniques (such as pumps) which bring the oil to the surface. These natural energy sources are: solution-gas drive, gas-cap drive, natural water drive, fluid and rock expansion and gravity drainage. The recovery factor in this first stage is usually low, it is possible to produce around 10% of a reservoir's oil in place.

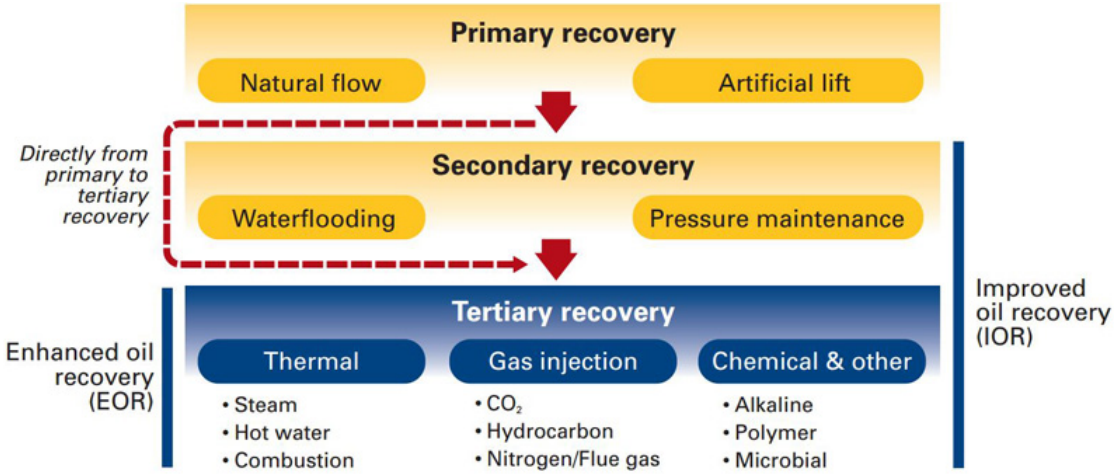

Figure 2.3: Oil recovery methods. [3]

2.3.2 Secondary Recovery

When the reservoir natural energies are not sufficient to produce, the secondary recovery is implemented. This stage consists in injecting water or gas to displace oil and drive it to a production well, resulting in the recovery of 20 to 40 percent of the original oil in place.

Therefore, the maximum value of recovery factor (primary + secondary recovery) is around 50 percent, but usually is around 35 percent. For this reason since the 70's, the producers have attempted several tertiary, or EOR techniques that offer prospects for ultimately producing 30 to 60 percent, or more, of the reservoir's original oil in place.

2.3.3 Tertiary Recovery / EOR methods

The ultimate goal of EOR processes is to increase the overall oil displacement efficiency, through increasing the capillary number and/or lowering the mobility ratio, compared to its waterflood value. Accordingly to equation 2.1, the interfacial tension between oil and water should be reduced, to increase the capillary number.

$$Nca = \frac{\nu \times \mu_w}{\sigma_{ow}} \tag{2.1}$$

$Where : Nca - capillary\ number; \nu - interstitial\ pore\ velocity;\ \mu_w - Water\ viscosity\ and\ \sigma_{ow} - Interfacial\ tension\ between\ oil\ and\ water.$

According equation 2.2, the mobility ratio is directly proportional to the oil viscosity and the relative permeability of the water and inversely proportional to the water viscosity and the relative permeability

of the oil. So, it is possible to decrease the mobility ratio by increasing water viscosity, reducing oil viscosity, reducing water permeability or all of the above.

$$M = \frac{\kappa_{rw} \times \mu_o}{\kappa_{ro} \times \mu_w} \tag{2.2}$$

$Where: M - mobility\ ratio; \kappa_{rw} - relative\ permeability\ of\ the\ water; \mu_o - Oil\ viscosity;$
$\kappa_{ro} - relative\ permeability\ of\ the\ oil\ and\ \mu_w - Water\ viscosity.$

Thus, the EOR categories to achieve the main goal are:

- **Thermal recovery**, which consists in decreasing the oil viscosity, through the steam injection, in-situ combustion, hot waterflooding, and others.
- **Gas injection**, which uses gases such as natural gas, nitrogen, or carbon dioxide (CO_2) that expand in a reservoir to push additional oil to a production wellbore, or other gases that dissolve in the oil to lower its viscosity and to improve its flow rate.
- **Chemical injection**, which can involve the use of long chained molecules called polymers to increase the water viscosity, and/or the use of detergent like surfactants to help lowering the interfacial tension that often prevents oil droplets from moving through a reservoir.
- **Others**, such as microbial processes and electromagnetic heating. [12, 13, 14]

2.4 Fluid displacement forces

Fluids flow on a porous media, like an oil reservoir, by the action of several forces. The most important forces are:

- Capillary forces,
- Gravity forces and
- Viscous forces

2.4.1 Capillary forces

The capillary forces have influence on oil recovery efficiency, which differs fundamentally for non-fractured and fractured reservoirs. In a non-fractured reservoir, if during the waterflooding the capillary forces are strong the oil will be trapped, and the residual oil saturation will be relatively high and the oil recovery will

be low. In fractured reservoirs, spontaneous imbibition of water due to strong capillary forces is regarded as an important and necessary mechanism to attain high displacement efficiency.

Capillary forces are frequently the strongest forces in a multiphase flow and the combination of all the active surface forces determines the capillary pressure in the porous rock. Due to tension between fluids' interfaces, there is a difference of pressure across the interface and this pressure is called capillary pressure, that is defined as the pressure of the non-wetting fluid minus the pressure of the wetting fluid.

2.4.2 Gravity forces

During an oil production process, the gravity force is very important, especially when a system has oil and gas with different densities between the fluid phases.

This force is also important when the interfacial tension between the oil and the water is low. Thus, in a system of immiscible fluids, this force is always present, making the lighter phase experience a pressure in upward direction.

2.4.2.1 Viscous forces

The viscous force is the force between a solid body and a fluid, liquid or gas. These forces in a porous medium are reflected in the magnitude of the pressure drop that occurs as a result of fluid flow through the medium. The viscous force is given by the multiplication of interstitial pore velocity and the fluid viscosity.

2.5 Wettability

Wettability describes the tendency of one fluid, known as the wetting phase, adhere to a solid, when other fluids are present. The wetting phase will tend to spread on the solid surface and the porous solid will tend to imbibe the wetting phase, displacing the nonwetting phase. [11]

This characteristic affects fluids saturation, capillary pressures, relative permeabilities, and oil recovery, thus its alteration was proposed as a method for improving oil recovery.

Regarding the wettability of a rock, it may be strongly water-wetting, strongly oil-wetting or intermediate wetting/neutral-wetting.

In a homogeneous porous material saturated with oil and water, the rock is strongly water-wetting if the surface strongly prefers contact with water, filling the smallest pores of the rock, and the oil is located in

the center of the larger pore, (Fig. 2.4a). In this case, the oil drops will be displaced from the center of the large pore, when performing the water flooding.

A strongly oil-wetting surface prefers contact with oil, which will cover most of the rock surface, occupying the smallest pores, and the water will be in the center of the larger pores, (Fig. 2.4c). In this case, when performing the water flooding, water mainly flows through the larger pore channels and the oil will remain stuck on the rock, occupying the smallest pores, where water does not penetrate.

When the solid does not have a preference for one fluid over the other, and both fluids tend to wet the solid, its condition is termed intermediate wetting or neutral-wetting, (Fig. 2.4b).

Therefore the wettability affects the quantity of oil that can be produced at the pore level, through the parameters S_{wi}, irreducible water saturation, and S_{or}, residual oil saturation, and influences the oil recovery.

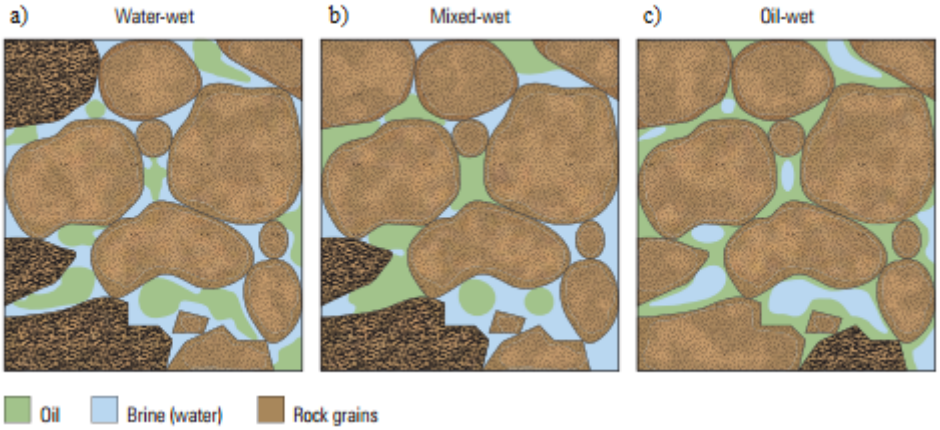

Figure 2.4: Wetting in pores. In a water-wet case (a), oil remains in the center of the pores, and the surface prefers contact with water. In a oil-wet (c), water remains in the center of the pores, and the surface prefers contact with oil. In the mixed-wet case, oil has displaced water from some of the surfaces, but is still in the centers of water-wet pores (b). [4]

It is possible to classify quantitatively the wettability through the contact angles, which is a function of the relative adhesive tension of the liquids to the solid, equation 2.3.

$$coseno\ \Theta = \frac{\sigma_{so} \times \sigma_{sw}}{\sigma_{wo}} \tag{2.3}$$

$Where:\ \theta - contact\ angle; \sigma_{so} - interfacial\ tension\ between\ the\ solid\ and\ oil; \sigma_{sw} - interfacial\ tension\ between\ the\ solid\ and\ water\ and\ \sigma_{wo} - interfacial\ tension\ between\ water\ and\ oil.$

The solid is water wet if the angle (θ) is less than 90° and oil wet if the angle (θ) is greater than 90°; the intermediate wettability occurs when the angle (θ) is around 90°.

In Fig. 2.5 the oil drop, in green, is surrounded by water, in blue. On a water-wet surface (a) the oil drop

forms a bead, and the contact angle is approximately zero. On an oil-wet surface (c), the drop spreads, and the contact angle is approximately 180°. And on an intermediate-wet surface (b), the oil drop also forms a bead, but the contact angle comes from a force balance between the interfacial tension terms, as show in equation 2.3. [4, 11]

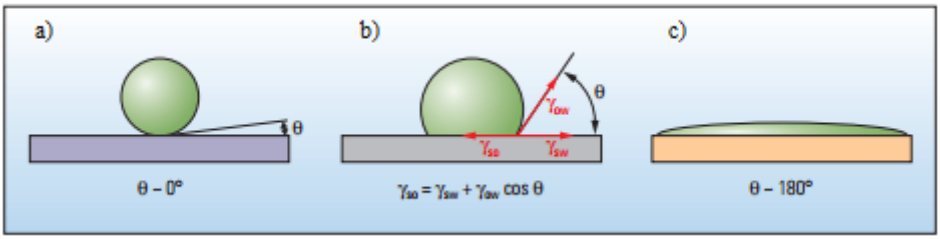

Figure 2.5: Contact angle. (a) represents a water-wet surface, the contact angle is approximately zero. (b) represents an oil-wet surface, the contact angle is approximately 180°. (c) represents an intermediate-wet surface. [4]

2.5.1 Wettability of carbonates

The majority of carbonate rocks have a tendency to be preferentially oil-wet, and recent studies have shown that carbonate reservoir rocks from the Middle East are generally neutral, mixed, or preferentially oil-wet, contrary to the sandstone reservoirs.

The wettability of a reservoir is an important parameter that affects fluid distribution, location and the flow of oil and water.

Carbonate reservoirs are fractured by nature, which is a challenge during production, because the injected water will flow through fractures to the production well, by passing most of the oil in the matrix blocks. If the rock is water wet, the water will imbibe spontaneously (process which one fluid displaces another from a porous medium, exclusively due to capillary forces) from the fractures into the matrix blocks and expel the oil through the fractures network. Due to negative capillary pressure, in a oil wet reservoir rock the spontaneous imbibition of water is not possible, and the oil remain in the matrix blocks.

Thus, the EOR potential for carbonates is very high due to presence of fractures, low displacement efficiency and unfavourable wetting conditions. [11, 15, 16]

2.6 Spontaneous imbibition

Spontaneous imbibition has been studied because of its importance in oil recovery from fractured reservoirs, with much emphasis on carbonate rocks.

Is an immiscible displacement process that describes the absorption of a wetting phase, with no pressure driving the phase into the rock, expect capillary forces. It is possible for the same rock to imbibe both water and oil, with water imbibing at low water saturation, displacing excess of oil from the surface of the rock, and oil imbibing at low oil saturation, displacing excess of water.

The rate of imbibition depends on several factors such as rock permeability, pore structure, wettability, and the interfacial tension between the resident fluid and the imbibing phase.

This way, imbibition is driven by surface energy, through the action of capillary force, where a non-wetting fluid within a porous medium, is spontaneously expelled by wetting fluid that surrounds the medium. This phenomenon is caused by the differential attraction forces between the pore walls and fluids. [17, 18]

2.7 Salinity as a wettability modifier

For many decades several studies were conducted in order to study the effect of injecting low salinity brine in oil recovery. In some cases when the injection brine salinity was substantially decreased the oil recovery increased.

The pioneering work was performed by Yildiz and Morrow in 1996 in sandstone and showed that, the ionic composition of the injected brine influenced the oil recovery. A few years later, in 2004 and 2005, Webb et al [5, 19]. shown an increased oil recovery from sandstones, by waterflooding with water of low salinity. (Fig. 2.6).

Since there are important differences between sandstone and carbonate rocks, currently studies have been extended to carbonate reservoir rocks.

As mentioned above carbonate rocks are preferentially oil-wet, and this characteristic occurs due to the adsorbing of carboxylic components present in crude oil onto the carbonate surface.

Strand et al. (2003) discovered that sulphate ions, SO_4^{2-}, present in the imbibing fluid act as a catalyst in the alteration of wettability. This discovery led to another work (Strand et al. 2006) that studies the potential of this ion as a wettablity alteration agent, using brine as the imbibing fluid. The conclusion shown that brine was able to alter the wetting of carbonate rocks and improve oil recovery.

In 2008 experimental studies done by Strand et al. showed that when injecting water ions, like sulphate SO_4^{2-}, calcium Ca^{2+} and magnesium Mg^{2+}, these became active ions in the wettability alteration process. [20]

Austad et al. and Strand et al. (2006) proposed a chemical mechanism for wettability alteration, illustrated in Fig. 2.7. When brine which contains a lot of SO_4^{2-} is injected into a reservoir, the SO_4^{2-} will adsorb onto the positively charged rock surface and the positive charge will decrease, leading to

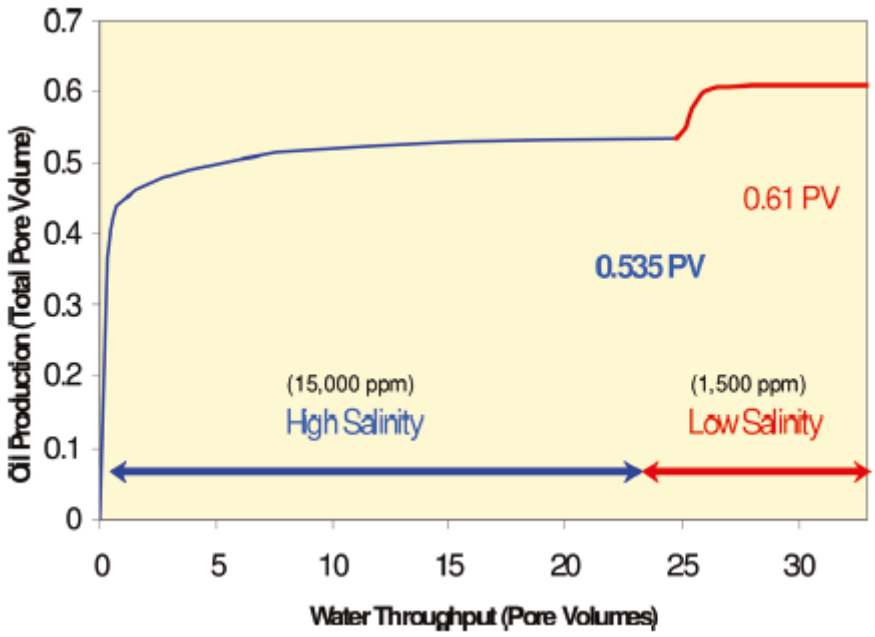

Figure 2.6: Oil production for high salinity vs. low salinity in sandstone. [5]

increased concentration of Ca^{2+} due to co-adsorption of this ion on the carbonate surface, since electrostatic repulsion is reduced. Thus, some of the strongly adsorbed carboxylic material is displaced from the surface, as Ca^{2+} reacts with negatively charged carboxylic groups bonded to the rock surface.

It is observed experimentally that SO_4^{2-} only acts as an important catalyst leading to an increase in the concentration of Ca^{2+} close to the surface. Austad et al. and Strand et al. (2006)suggest that Mg^{2+} can substitute Ca^{2+} at rock surface, when the this ion is connected to the carboxylic group, which means that Mg^{2+} is able to displace Ca^{2+} ions from the surface, as showed in Fig. 2.7B. Also, this reaction is catalysed by SO_4^{2-}. The combined effects make the rock surface to be less oil-wet. [6, 21, 22]

In this work, it is experimentally verified that the interactions between the active components, SO_4^{2-}, Ca^{2+} and Mg^{2+}, dissolved in water and the rock surface are responsible for the improvement in water wetness of carbonate rocks. In addition is also demonstrated that with high temperatures, the affinity of (SO_4^{2-}) to rock surface increases (Strand et al., 2006).

Thus, the capacity of brine to act as a wettability modifier in an oil-wet rock depends on the ions present and the temperature, and once the potential ions are not present in the brine, it can be modified to contain these ions in proper concentration in order to improve oil recovery. [23, 24, 25, 26, 27, 28, 29]

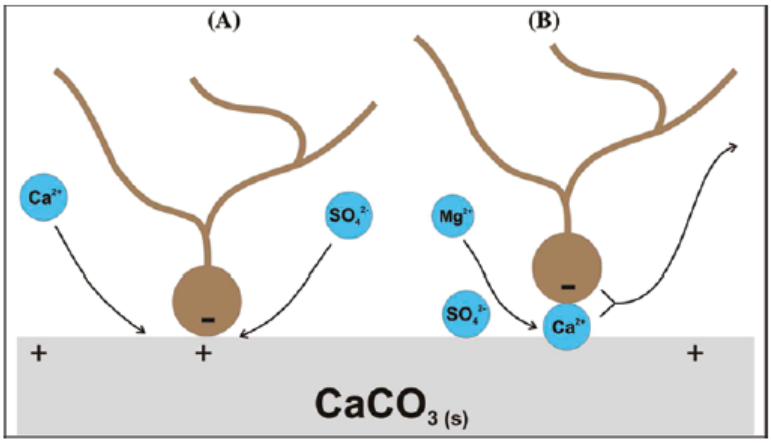

Figure 2.7: Suggested mechanism for the wettability alteration induced by seawater. A: Proposed mechanism when Ca^{2+} and SO_4^{2-} are the active species. B: Proposed mechanism when Ca^{2+}, Mg^{2+} and SO_4^{2-} are active at high temperatures. [6]

2.8 Literature Review Summary

The main objective of this work is to increase the oil recovery in Carbonate Reservoirs. To achieve this goal it is necessary to change the rock wettability, since carbonate rocks are preferentially oil-wet making difficult the oil recovery.

Is possible to improve the oil recovery through water injection with different salinity and ionic composition. The brine composition have three principal active ions that contribute for the wettability alteration, sulphate, calcium and magnesium. When the concentration of non-active ions is reduced, the salinity is reduced, and the active ions (SO_4^{2-}, Ca^{2+} and Mg^{2+}) have easier access to the rock surface, making the rock less oil-wet.

When a brine which contains a lot of SO_4^{2-} is injected, this ion will be adsorbed on the positively charged surface and the positive surface charge will decrease, leading to increased concentration of Ca^{2+} due to co adsorption of this ion on the carbonate surface, since electrostatic repulsion is reduced. By this, some of the strongly adsorbed carboxylic material is displaced from surface, as Ca^{2+} reacts with negatively charged carboxylic groups bonded to the rock surface. The fact that the experiment is performed at elevated temperature, 120 °C, also contributes to improve oil recovery.

So, it is expected that during the experiment when brine is injected with reduced concentration of non active ions and high concentration of sulphate, or others active ions, the wettability of the limestone core will change, becoming less oil-wet, and allowing the oil displacement from the rock surface.

Chapter 3

Material

This chapter describes the most important material used during the experiment. It is organized as follows:

- **Section 3.1** presents the characteristics of the cores used in the experiment.
- **Section 3.2** describes the properties of the oil used in the laboratory, and also presents a comparison between these properties and the ones founded in field.
- **Section 3.3** describes the characteristics of the brines used in the experiment.
- **Section 3.4** lists in detail the most important equipment used.
- **Section 3.5** shows the main differences between the laboratory conditions and field conditions.

3.1 Cores

In the reservoir under study the target formation is made of limestone, for this reason the cores used in the experiment are Indiana limestone, see Fig. 3.8. The cores used are from outcrops, which means they are not from the reservoir, but from the surface. At each core is assigned the code CC and a number, between 1 and 4.

The first step consisted on cutting the cores, with appropriate measures for the realization of the experiment. Therefore, for this study 4 cores were used (see Fig.3.8) with different characteristics, as shown in Table 3.2.

The core absolute pore volume (PV) has been calculated from the difference between the core weight when it is saturated with degassed brine, and the core weight when it is completely dried, divided by

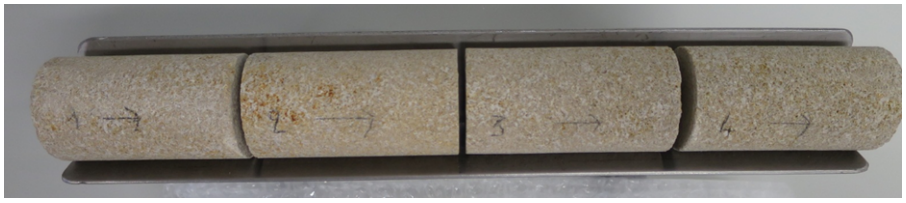

Figure 3.8: Limestone cores

Core	Length (mm)	Diameter (mm)	Dry Weight (gr)	Pore Volume (PV) (mL)	Bulk Porosity ($\%$)
1	69.77	38.07	171.619	15.9	20.02
2	73.92	38.08	181.439	16.9	20.07
3	73.81	38.07	180.805	17.1	20.35
4	73.66	38.08	181.799	16.6	19.79

Table 3.2: Characteristics of Limestone cores

water density value, 1 g/ml. This value corresponds to the water that has come into the core.

Pore volume equation:

$$PV = Core\ weigth\ after\ water\ saturation - Core\ weigth\ before\ water\ saturation \tag{3.4}$$

Absolute porosity has been calculated as the relation between the pore volume and the core total volume.

The most basic property of reservoir rocks is porosity, the percentage of pore volume or void space, or that volume within rock that can contain fluids (gas, oil, and water).

The total volume of fluid that can be stored in a given bulk volume of rock is its pore volume. The bulk volume, of the rock is the sum of the grain and pore volumes. The total, or absolute porosity, is the pore volume divided by the bulk volume (expressed as percentage), equation 3.5.

$$\phi\ (\%) = \frac{V_p}{V_b} \tag{3.5}$$

$Where: \phi - Porosity;\ V_p - Pore\ volume\ and\ V_b - Bulk\ Volume\ of\ Rock$

3.2 Oil

An oil with similar characteristics as the crude analysed in the oil field was chosen, as follows:

- **Crude oil API gravity:** 38.88° at 15.5 °C
- **Percentage of Sulfur:** 1.28 %

- **Crude oil density:** 0.81672 *kg/l* at 40 °C

Its viscosity was measured at several temperatures, 15 °C, 24 °C, 30 °C, 40 °C, 50 °C, 60 °C and 70 °C, using a Rheometer, at the shear rate of 50 s^{-1}. A Rheometer is a laboratory equipment used to measure how a liquid flows in response to applied forces. However, it was not possible to measure the oil viscosity at reservoir temperature, because this temperature is very high and same components of the oil may evaporate. However, it is possible to calculate the viscosity at 120 °C, by applying Arrhenius equation, 3.6.

$$\mu = \mu_0 \times \exp \frac{E}{RT} \tag{3.6}$$

$Where: \mu - dynamic\ viscosity;\ \mu_0 - viscosity\ at\ reference\ temperature;\ E - temperature\ coefficient\ for\ viscosity;\ R - universal\ gas\ constant\ and\ T - temperature.$

To calculate the viscosity at 120 °C, was used a graph based on Arrhenius equation (Fig. 3.9), where x is the inverse of temperature in Kelvin degrees and y is the viscosity.

In this graph, the points represent the values of viscosity measured at different temperatures, and the exponential function is the one that best fits these points. Therefore, it is possible to retrieve the viscosity value of the reservoir oil from the plot using reservoir temperature.

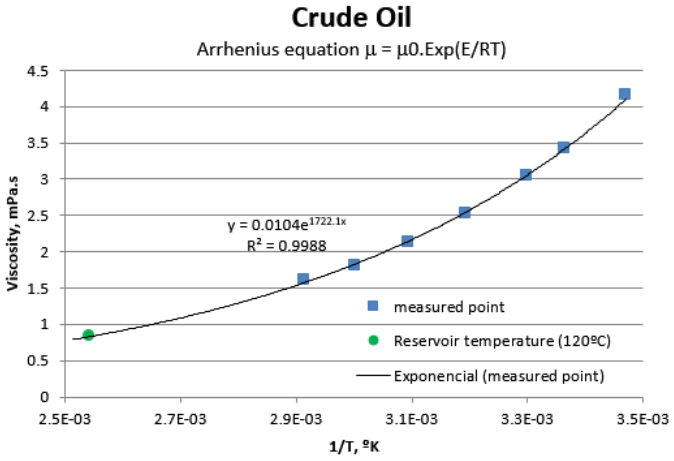

Figure 3.9: Oil viscosity

Thus the results of oil viscosity from the Rheometer and from Arrhenius equation are shown in Table 3.3.

Temperature (°C)	viscosity ($mPa.s$)
15	4.15
24	3.425
30	3.04
40	2.52
50	2.13
60	1.81
70	1.607
120	0.831

Table 3.3: Oil viscosity

3.3 Brines

During the experiment different brines were prepared such as: Formation Brine (FB), Synthetic Seawater (SSW), Synthetic Seawater diluted 10 times (SSW 1/10), Synthetic Seawater diluted 25 times (SSW 1/25) and Synthetic Seawater modified (SSW mod). The salts used to prepare the fluids included: $NaCl$, $CaCl_2.2H_2O$, $MgCl_2.6H_2O$, $NaHCO_3$, Na_2SO_4 and KCl. KCl was used in all brines expect FB. The necessary weight of the different types of salts were added to tap water, since the amount of salt present in this water was negligible. The salts were added one by one, beginning with the salt that had the largest amount and ending with the salt in smallest amount. Once added the first salt, the water with the salt was stirred with s magnetic stirrer, and when the mixture was homogeneous another salt was add, until all the brine composition was complete. Then, the brine was filtered through a 0.22 μm filter to remove possible particles that were undissolved.

For each one, except for SSW mod, the viscosity and density were measured at different temperatures and at reservoir temperature. The pH was also measured to monitored if the water characteristics are not changed after injection.

The viscosity (resistance to flow) was measured in all synthetic brines at reservoir temperature. The first step was to measure density and the synthetic brine kinematic viscosity, using an Ubbelohde capillary, for 24 °C, 40 °C and 50 °C, respectively.

The Ubbelohde viscometer is used to determine kinematic viscosity of transparent liquids. The brine was introduced in the equipment and then sucked using a suction bulb, making the liquid passing through the capillary and the two calibrated marks. Then the suction bulb is removed and the liquid travels back.

To calculated kinematic viscosity of the sample, the efflux time is multiplied by the viscometer constant, 3.7:

$$\nu = Efflux\ time \times\ coefficient \tag{3.7}$$

$Where: \nu - kinematic\ viscosity;\ Efflux\ time - time\ it\ takes\ for\ the\ sample\ to\ pass\ through\ two\ calibrated\ marks;\ and\ coefficient - viscosimeter\ constant.$

After this step, the equation 3.8 was applied, to determine the brine viscosity for each temperature.

$$\mu = \nu \times \rho \tag{3.8}$$

$Where: \mu - dynamic\ viscosity;\ \nu - kinematic\ viscosity;\ and\ \rho - density.$

The Arrehnius equation (equation 3.6) was used to determine the brines' viscosity at reservoir temperature (120°C), as explained for the case of oil samples.

3.3.1 Formation Brine

The synthetic FB was prepared according to the features of FB analysed in the field, as shown in Table 3.4.

Composition	Brine from the oil field (mg/L)	Synthetic FB after filtration (mg/L)
Chloride	114363.17	108186.24
Sulphate	273.33	281.02
Carbonate	NL	-
Bicarbonate	368.00	-
Calcium	16666.67	16798.84
Magnesium	1570.00	1586.08
Iron	135.00	-
Sodium	52235.67	57542.42

Table 3.4: Comparison between FB from the oil field and synthetic FB

The Total Dissolved Solids (TDS) for synthetic FB was 229 *g/L*.

The viscosity values for synthetic FB, determined as described above are, shown in Table 3.5:

Temperature (°C)	Density (g/cm^3)	Kinematic viscosity (mm^2)	Viscosity ($mPa.s$)
24	1.139	1.03858	1.183
40	1.131	0.77091	0.872
50	1.126	0.69992	0.788
100	-	-	0.411
120	-	-	0.333

Table 3.5: Characteristics of synthetic FB

In the end, the solution pH was measured using a pH meter, and this value after filtration was 6.5.

3.3.2 Synthetic Sea water

The SSW was prepared according the results of the analysis performed over seawater samples.

Once this brine was prepared, an analysis to quantify the anions and cations present and verify that the preparation was well made, was performed. A comparison between the original and the prepared seawater composition is presented at Table 3.6.

Composition	Sea water (mg/L)	SSW after filtration (mg/L)
Chloride	20128.40	19466.46
Sulphate	2743.03	2756.76
Calcium	470.54	499.71
Magnesium	1329.86	1363.19
Sodium	11156.87	10951.09
Potassium	350.33	373.09

Table 3.6: Comparison between Sea water and SSW

The TDS was 42 *g/L*.

The results of the laboratorial procedure to determine the viscosity are shown in Fig. 3.10 and Table 3.7.

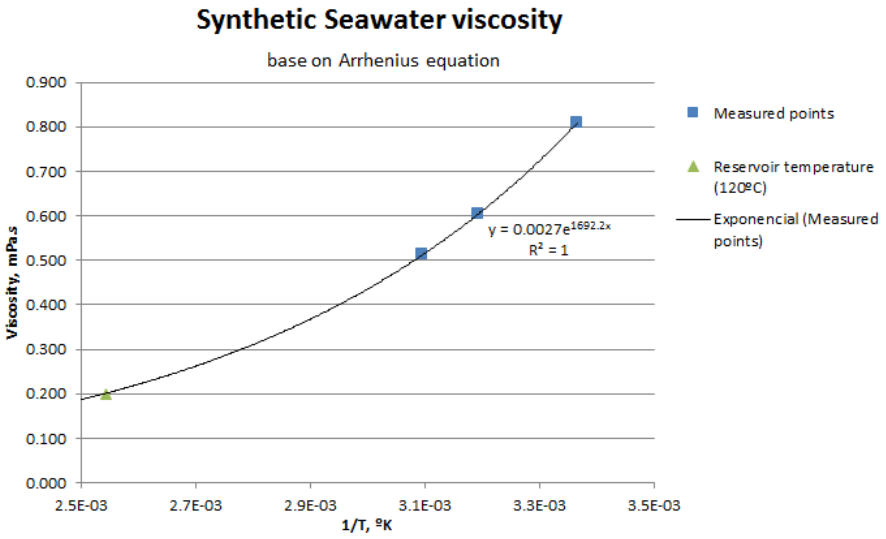

Figure 3.10: SSW viscosity

Temperature (°C)	Density (g/cm^3)	Kinematic viscosity (mm^2)	Viscosity ($mPa.s$)
24	1.0253	0.7891	0.809
40	1.0185	0.5929	0.604
50	1.0135	0.5050	0.512
100	-	-	0.252
120	-	-	0.200

Table 3.7: Characteristics of SSW

The solution pH was also measured using a pH meter, and this value after filtration was 6.3.

3.3.3 Synthetic Sea water diluted 1/10

The SSW 1/10 was obtained by diluting ten times the SSW previously prepared. Once prepared, this brine was analysed, to quantify the anions and cations present, and to verify if it complied with the theoretical composition, (Table 3.8).

Composition	SSW 1/10 theoretical composition (mg/L)	SSW 1/10 composition after filtration (mg/L)
Chloride	2012.84	2060.13
Sulphate	274.30	289.41
Calcium	47.05	45.34
Magnesium	132.99	127.16
Sodium	1115.69	1054.71
Potassium	35.03	35.49

Table 3.8: Comparison between SSW 1/10 theoretical composition and SSW 1/10 composition after filtration

The TDS was 4.2 *g/L*.

The results of the laboratorial procedure to determine the viscosity are shown in Fig. 3.11 and Table 3.9.

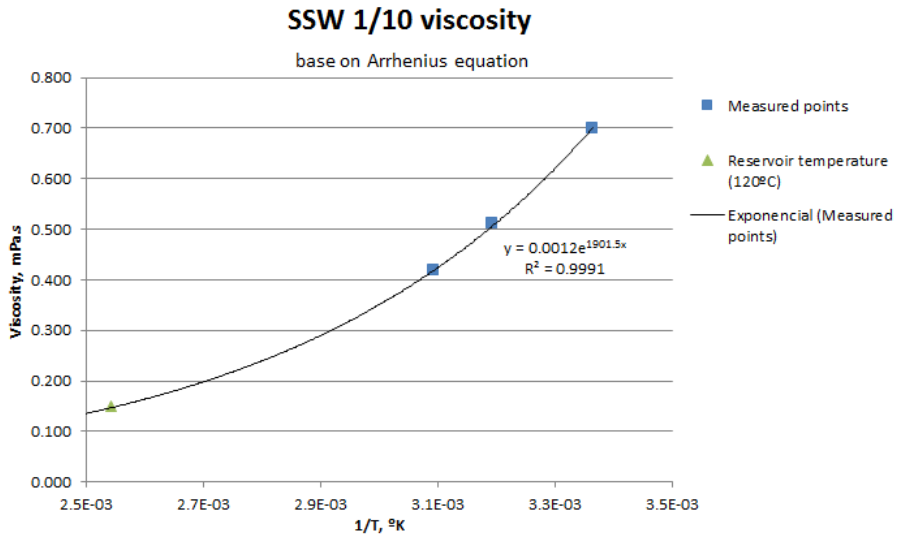

Figure 3.11: SSW 1/10 viscosity

Temperature (°C)	Density (g/cm^3)	Kinematic viscosity (mm^2)	Viscosity ($mPa.s$)
24	1.0011	0.6989	0.700
40	0.9949	0.5134	0.511
50	0.9907	0.4210	0.417
100	-	-	0.196
120	-	-	0.151

Table 3.9: Characteristics of SSW 1/10

The pH solution was 6.3.

3.3.4 Synthetic Sea water diluted 1/25

The SSW 1/25 was obtained by diluting twenty five times the SSW previously prepared. Once prepared, this brine was analysed, to quantify the anions and cations present, and to verify if it complied with the theoretical composition (Table 3.10).

Composition	SSW 1/25 theoretical composition (mg/L)	SSW 1/25 composition after filtration (mg/L)
Chloride	805.14	813.68
Sulphate	109.72	109.56
Calcium	18.82	18.28
Magnesium	53.19	64.00
Sodium	446.27	493.69
Potassium	14.01	18.28

Table 3.10: Comparison between SSW 1/25 theoretical composition and SSW 1/25 composition after filtration

The TDS was 1.7 *g/L*.

The results of the laboratorial procedure to determine the viscosity are shown in Table 3.11.

Temperature (°C)	Density (g/cm^3)	Kinematic viscosity (mm^2)	Viscosity ($mPa.s$)
24	0.9994	0.6966	0.696
40	0.9934	0.5151	0.512
50	0.9887	0.4484	0.443
100	-	-	0.217
120	-	-	0.172

Table 3.11: Characteristics of SSW 1/25

The pH solution was 7.8.

3.3.5 Synthetic Sea water modified

The brine SSW mod was prepared by modifying the SSW, decreasing the $NaCl$ concentration twice and increasing the Na_2SO_4 concentration four times.

Once prepared, this brine was analysed, to quantify the anions and cations present, and to verify if it complied with the theoretical composition, (Table 3.12).

Comparing the values presented in Table 3.12, the SSW mod theoretical composition and SSW composition after filtration is different, however the difference is not high and can be negligible.

The SSW mod TDS was about 42.4 *g/L*, which was similar to SSW value (42 *g/L*).

The pH solution was 7.9.

Composition	SSW mod theoretical composition (mg/L)	SSW mod composition after filtration (mg/L)
Chloride	12854.48	16278.63
Sulphate	11023.53	13303.44
Calcium	624.75	619.60
Magnesium	1329.38	1539.62
Sodium	10312.09	12495.31
Potassium	354.84	516.33

Table 3.12: Comparison between SSW mod theoretical composition and SSW mod composition after filtration

3.3.6 Brines summary

To summarized is presented in Table 3.13 the characteristics of the brines prepared with ionic composition, TDS, pH and viscosity.

Ions	FB	SSW	SSW 1/10	SSW 1/25	SSW mod
Chloride, *mg/L*	108186.24	19466.46	2060.13	813.68	16278.63
Sulphate, *mg/L*	281.02	2756.76	289.41	109.56	13303.44
Calcium, *mg/L*	16798.84	499.71	45.34	18.28	619.60
Magnesium, *mg/L*	1586.08	1363.19	127.16	64.00	1539.62
Sodium, *mg/L*	57542.42	10951.09	1054.71	493.69	12495.31
Potassium, *mg/L*	-	373.09	35.49	18.28	516.33
TDS, *g/L*	229	42	4.2	1.7	42.4
pH	6.5	6.3	6.3	7.8	7.9
Viscosity, *mPa.s*	0.333	0.200	0.151	0.172	-

Table 3.13: Summaries of brines characteristics

3.4 Equipment

The list of material used during the experiment is long and very varied, some of them are volumetric flasks, ovens, pumps, salts used to prepare the brines, coreholders and others.

To obtain brines with good characteristics, the material used is presented below:

- **Salts**

  The salts used in brines preparation are $NaCl$, $CaCl_2.2H_2O$, $MgCl_2.6H_2O$, $NaHCO_3$, Na_2SO_4 and KCl.

- **Magnetic stirrer**

  To ensure a homogeneous mixture the brines are stirred in a magnetic stirred, Fig. 3.12a, until all the salts are dissolved.

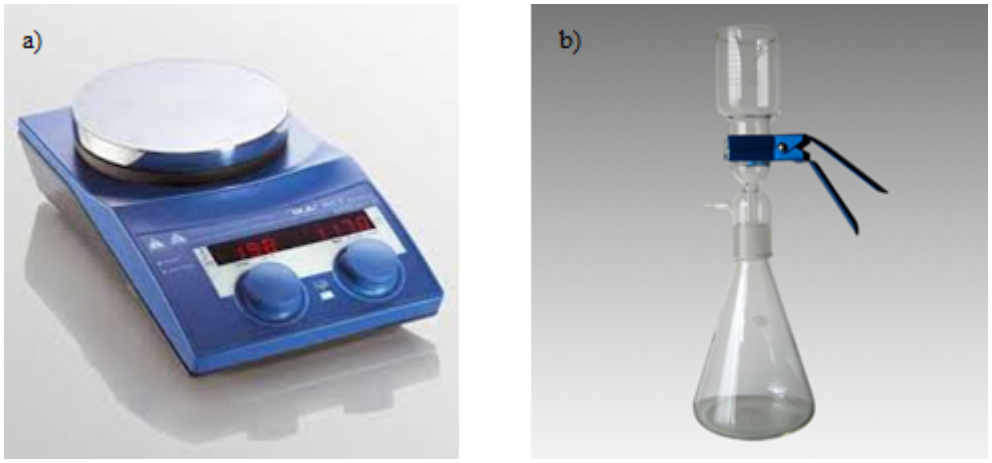

Figure 3.12: (a) magnetic stirrer and (b) filtration set-up

- **Filters**

  After stirring the brines are filtrated to ensure that undissolved particles are removed. Undissolved particles can block the pores in the core. To filtrate the brines 0.22 μm filters were used. The filtration set-up is presented in Fig. 3.12b.

- **Ubbelohde viscometer**

  Ubbelohde viscometers are used to determine kinematic viscosity of transparent liquids. A liquid is introduced into the equipment and then sucked using a suction bulb, making the liquid passing through the capillary and the two calibrated marks. Then the suction bulb is removed, the liquid travels back, and the time that the liquid takes to pass through the two calibrated marks is the efflux time, that multiplied by the viscometer constant, gives the value of kinematic viscosity. The Ubbelohde viscometer have also a third arm extending from the end of the capillary and open to the atmosphere, Fig. 3.13. This device was invented by the German chemist Leo Ubbelohde (1877-1964).

- **Thermal bath**

  To measure the kinematic viscosity at 40 °C and 50 °C a Thermal bath, designed for basic laboratory heating applications, was used. Therefore, to measure the kinematic viscosity, the Ubbelohde viscometer was immersed in the bath, as well as the liquid inside the Ubbelohde viscometer. When the thermal bath and the sample reach the desired temperature the kinematic viscosity at different temperatures can be measured.

- **Rheometer**

  A rheometer is an instrument used for measuring the rheological properties of a substance. In this case, to measure how a liquid flows in response to applied forces.

Figure 3.13: Ubbeholde viscometer

- **Desiccator**

  To measure the pore volume, the core is dried, weighted and placed inside the desiccator, (Fig. 3.14a). When there is no more air in the pores, the desiccator is filled with degasified brine, to saturate the pores, as shown in Fig. 3.14 b.

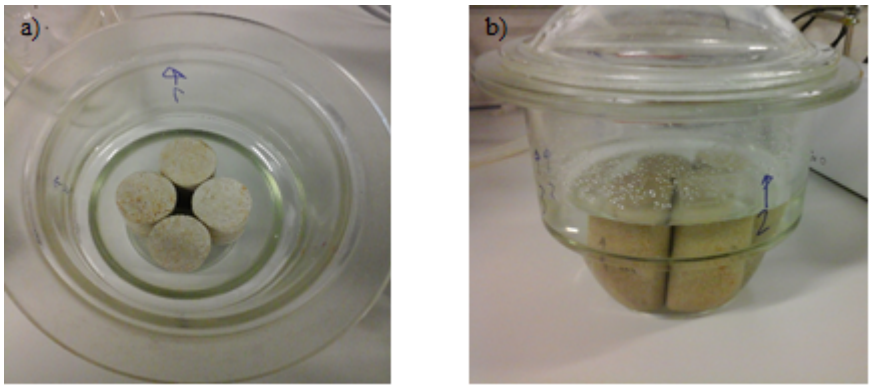

Figure 3.14: (a) desiccator with dried cores and (b) desiccator when the cores are getting saturated with brine

- **Vacuum flask** or **Büchner flask**

  Before using a brine, it needs to be degassed, to avoid air presence inside the core. Thus, the brine is placed in a vacuum flask, closed and the air is removed through a balloon with helium and vacuum.

- **Coreholder**

  For the experiment realization, the core needs to be placed in a coreholder, Fig 3.15. Coreholder

is the equipment employed to confine the core and simulate the reservoir conditions. The core is situated inside a rubber sleeve and completely isolated. Between the external face of the sleeve and the internal face of the coreholder there is a hollow space which is filled with a silicone oil, to apply confining pressure. In this experiment the confining pressure was 40 *bar*.

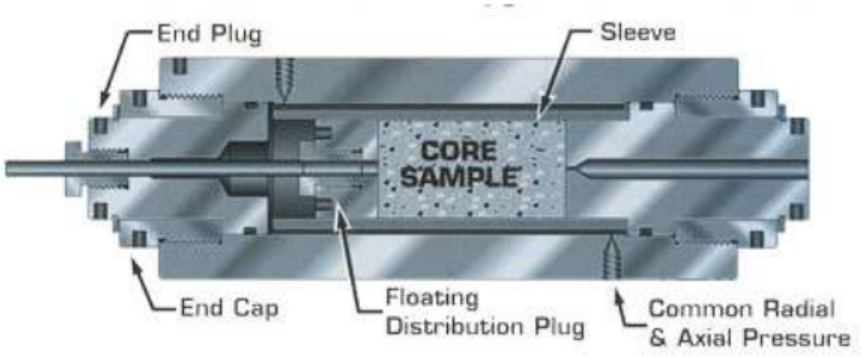

Figure 3.15: Coreholder diagram. [7]

- **Online UV detector**

  The online UV detector measures the absorbance at 280 nm. When an ultraviolet tracer is injected in a flow of brine that is injected in a core, this equipment allows to know the time that the tracer needs to pass through the core and knowing the flow rate it is possible to calculate the pore volume of the core.

- **Pumps: ISCO 500D**, **Quizix QX** and **Pharmacia LKB Pump P-500**

  During the experiment different types of pumps were used for different applications. This equipment is very important, because it allows to inject into the core the desired fluid with the right pressure and flow rate.

  The main pump used to inject the fluids into the core was Quizix QX pump, Fig. 3.16a. This kind of pump is made of hastelloy, a material very resistant to corrosion, and can inject two different fluids at high pressure, providing very accurate rate control.

  The other pump most often used, was an ISCO 500D piston pump, Fig. 3.16b. This pump is also made of hastelloy, in similarity to the Quizix QX pump, it can inject at high pressure and provides a very accurate rate control, however this pump have just one piston.

  An auxiliary pump also used, was a Pharmacia LKB Pump P-500, Fig. 3.16c. This kind of pump is very resistant and they can inject at high pressure also, however its pressure and rate control is not very accurate, due to the need to change piston during injection which leads to a pressure drop.

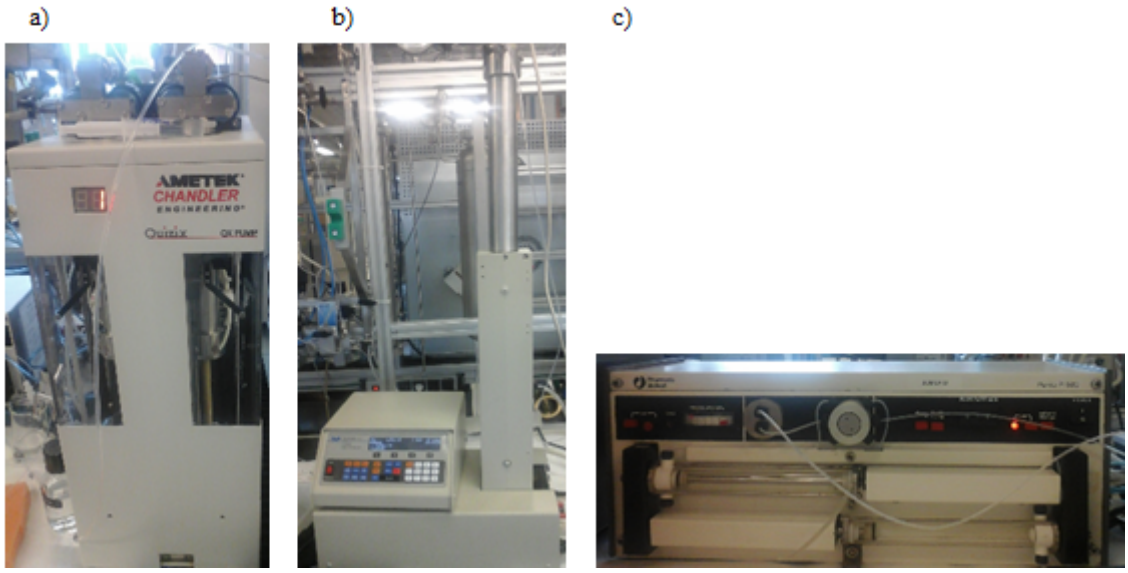

Figure 3.16: (a) a Quizix QX pump, (b) an ISCO 500D pump, and (c) a Pharmacia LKB Pump P-500

- **Digital mass flow meter/Controller**

  In this experiment the digital mass flow meter used is a mini CORI-FLOW, presented in Fig. 3.17. This instrument allows accurate measurements and control of low flow rates.

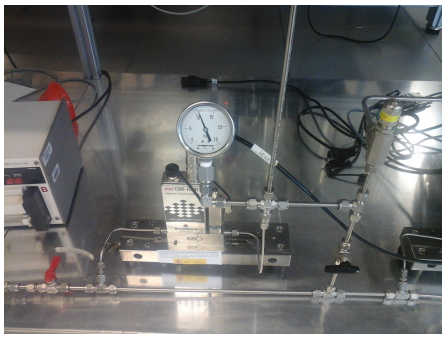

Figure 3.17: Digital mass flow meter

- **Ceramic disc**

  The ceramic disc is very important for the setup, it allows water to passing through it, but not oil.

- **BPR (Back Pressure Regulator)**

  A BPR, Fig. 3.18, is a pressure control that keeps the pore pressure at the desired value, and at the same time keeps the fluid from boiling and evaporating at high temperature. This experiment was performed with back pressure of 10 *bar*.

- **Pressure transmitter**

Figure 3.18: Back pressure regulator

A pressure transmitter measures pressure. This device allows the control and monitoring of the inlet and the outlet pressure. The DP (Differential Pressure), is given by the difference between inlet and outlet pressure and the DP value should be positive. The pressure transmitters are presented in Fig. 3.19.

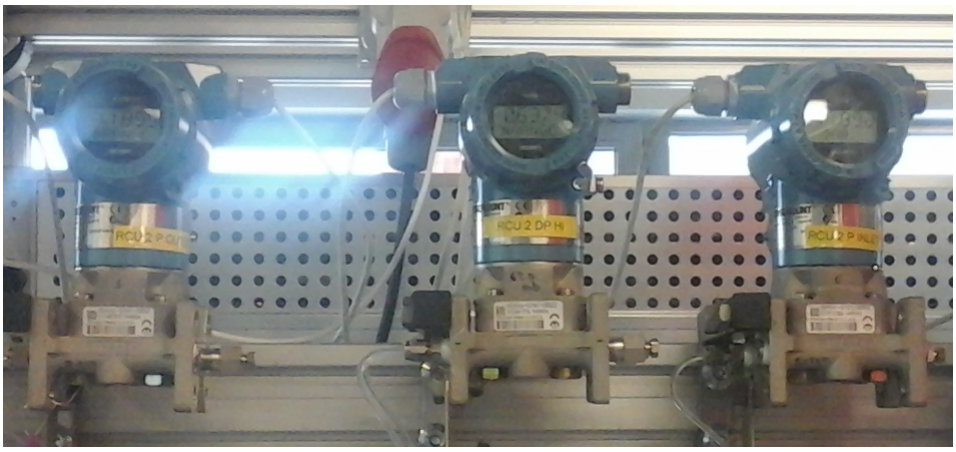

Figure 3.19: Pressure transmitters

- **Oven**

  During the experiment different ovens were used for each phase. Ovens are an important part of the set up, as they are used to keep the coreholder at reservoir temperature.

- **High pressure burette**

  An high pressure burette, Fig. 3.20a, was used to collect the first injection effluent.

- **Sample collector**

  A sample collector, Fig. 3.20b, was also used to collect injection effluent. This collector is ideal for automatic collection, it can collect until 80 samples, using a frequency time that can be set up.

- **pH-meter**

  Finally, to measure the pH a ph-meter Mettler Toledo was used.

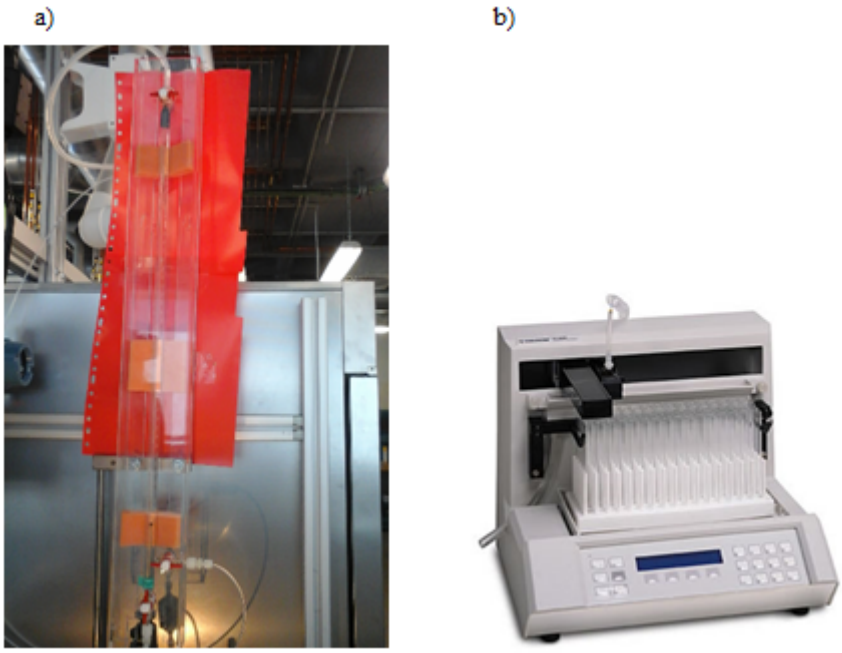

Figure 3.20: (a) high pressure burette and (b) sample collector

3.5 Summary

The field conditions and laboratory conditions are summarized in Table 3.14.

	Field conditions	Laboratory conditions
Reservoir temperature (°C)	120	120
Reservoir rock	Limestone	Indiana limestone
Porosity (%)	11-28	18.5
Oil °API at 15.5 °C	35.6	38.88
Oil density at 40 °C	0.8292	0.8167
Oil viscosity at 120 °C (*mPa.s*)	1.07	0.831
FB salinity, (*g/L*)	229	229
FB viscosity at 120 °C, (*mPa.s*)	NA	0.333
SSW salinity, (*g/L*)	NA	42
SSW viscosity at 120 °C, (*mPa.s*)	NA	0.200

Table 3.14: Field conditions vs. Laboratory conditions

Chapter 4

Experimental methodology

This chapter describes all the steps needed in order to prepare a core for a EOR core flooding experiment.

The chapter is organized as follow:

- In **Section 4.1** a chapter introduction is made.
- **Section 4.2** presents the different units and procedures used during the core preparation, and the results achieved.
- **Section 4.3** describes the different units and methodology used during the core flooding.
- **Section 4.4** summarises the chapter.

4.1 Introduction

An EOR core flooding experiment at reservoir temperature has three principal steps: the core cleaning, core saturation and core flooding.

In order to perform an experiment of EOR core flooding it is important to reproduce the reservoir conditions in the core, like fluids saturation and wettability. For this purpose, first the core must be carefully cleaned of any rest of oil, perforation fluids, water, salts, or any other additives that it may contain.

Afterwards, the core is placed in a coreholder, that is used to confine the core and simulate the reservoir conditions.

Then, different measurements can be done in order to characterize the rock to be used during the experiments. In the saturation step, the core is saturated with the original fluids, crude oil and reservoir

brine, and then submitted to ageing process.

Therefore, the main steps in the preparation of a core are:

- Gas permeability measurement at normal and reverse flow, at ambient temperature;
- Water saturation;
- Water permeability measurement at normal and reverse flow, at ambient temperature and at reservoir temperature;
- Dynamic pore volume measurement;
- Crude oil saturation;
- Irreducible water saturation measurement;
- Ageing at reservoir temperature;
- Crude oil injection at ambient temperature;
- Ageing at reservoir temperature;
- Injection of brines with different salinity.

4.2 Core preparation methodology

4.2.1 Units

During core preparation there were two fundamental units, the oil saturation unit and the ageing unit, that are presented in detail below.

4.2.1.1 Oil saturation unit

In the oil saturation unit, Fig. 4.21, the main objective is to saturate with oil the core until Swi is reached.

Thereby, to achieve this goal, oil is injected at ambient temperature and at different pressure steps, namely 0.5 *bar*, at 1 *bar*, at 2 *bar*, at 4 *bar*, at 6 *bar*, at 8 *bar* and at 10 *bar*, the maximum oil pressure limit allowed. A ceramic disc permeable to water but not to oil, is placed at the outlet of the core, allowing the water to come out when oil is injected, but keeping the oil inside. The volume of water produced is measured at the outlet using a burette (Fig. 4.21).

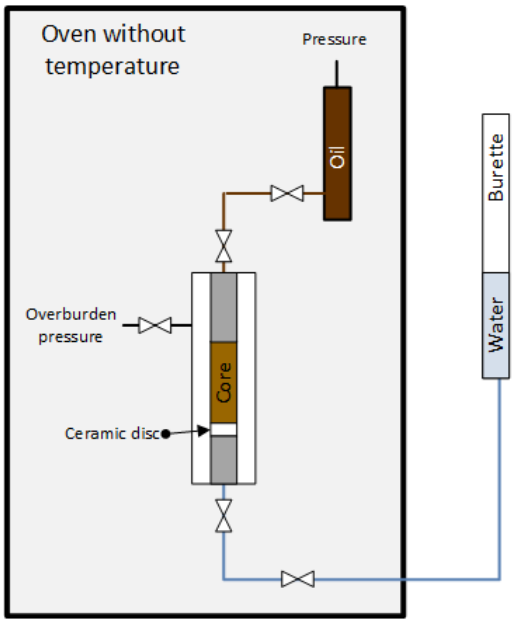

Figure 4.21: Oil saturation unit

4.2.1.2 Ageing unit

The purpose of the ageing procedure is to make fluids adhere to the rock and this way restore the real wettability present in the field. To achieve this purpose the time of ageing should be, at least, two weeks.

Therefore, once the core is saturated with oil, the coreholder with respective core is placed in the ageing unit. There, relative rock permeability to oil is measured by injecting a fresh slug of oil into the core, at different flow rates namely, 2 *ml/hr*, 10 *ml/hr*, 25 *ml/hr*, 50 *ml/hr*, 100 *ml/hr* and 0 *ml/hr* to correct previous values.

In the apparatus of Fig. 4.22, the oil is going inside the coreholder, and respective core, from below and going out from above. The cylinder has a piston that separates water from oil, and the water is inject from below with different flows and using the flow transmitter. When the water is injected in the cylinder the oil comes out from above and goes into the core. In the assembly, the BPR prevents the fluids of boiling and evaporating at high temperature, and the flow transmitter, placed outside the oven, allows the control of the injected flow rate.

4.2.2 Measurement of rock permeability to gases

The first parameter usually measured in order to characterize a rock is the permeability. The permeability to gases is measured by monitoring the DP. In this case, the permeability was measured with a confining pressure of 20 *bar* in normal and reverse flow with Nitrogen (viscosity = 0.01777 *mPa.s* or *cP*).

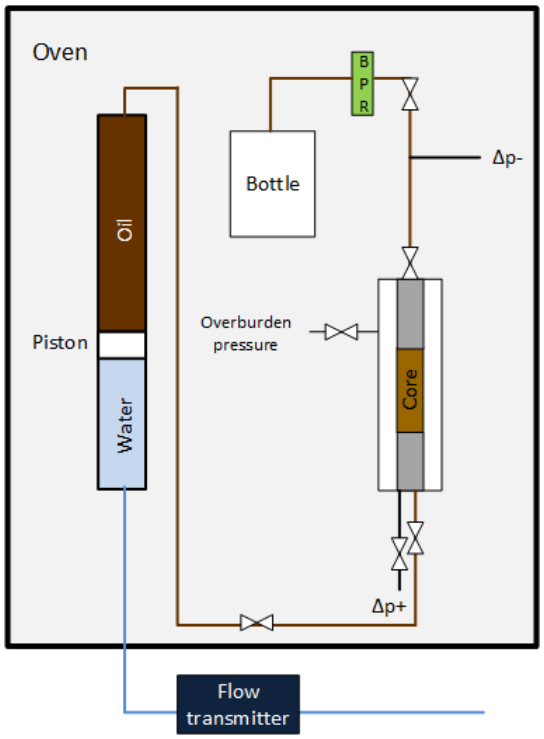

Figure 4.22: Ageing unit

The first step before starting the procedure is to dry the core. For this, the core is kept in an oven at 80 °C, overnight. The next step is to place the core in the coreholder and apply the confining pressure. Then, at ambient temperature, the gas is injected. Using a gas meter the gas flow is monitored, as well as the differential pressure along the core, with the outlet at atmospheric pressure. The gas volume that went through the core during a specific time is used to calculate the gas flow rate.

The permeability was estimated using equation 4.9, after measuring the pressure produced in the core at different flow rates.

$$\kappa(mDarcy) = 2 \times \frac{\mu(cP) \times L(cm)}{S(cm^2)} \times \frac{Q(cc/h) \times P(bar)}{(P_1^2 - P_2^2)(bar^2)} \times 1013 \tag{4.9}$$

$Where : \kappa - permeability; \mu - fluid\ viscosity; L - Lenght\ of\ the\ core; S - area\ of\ the\ core; Q - flow\ rate; P - absolute\ pressure\ for\ the\ flow\ rate\ measurement; P_1 - absolute\ pressure\ on\ the\ inlet\ and\ P_2 - absolute\ pressure\ on\ the\ outlet$

4.2.2.1 CC-01

For the calculations of core number 1, equation 4.9 was applied, where μ is 0.01777 cP; L is 6.977 cm; S is 11.38 cm^2, since the core diameter is 3.807 *cm*; P and P_2 are the atmospheric pressure, 1.013 *bar*;

P_1 varies in accordance with the DP; and Q varies in accordance with the gas volume and time.

The relation between $(P_1^2 - P_2^2)/P$ and the flow rate (Q) is presented in Fig. 4.23.

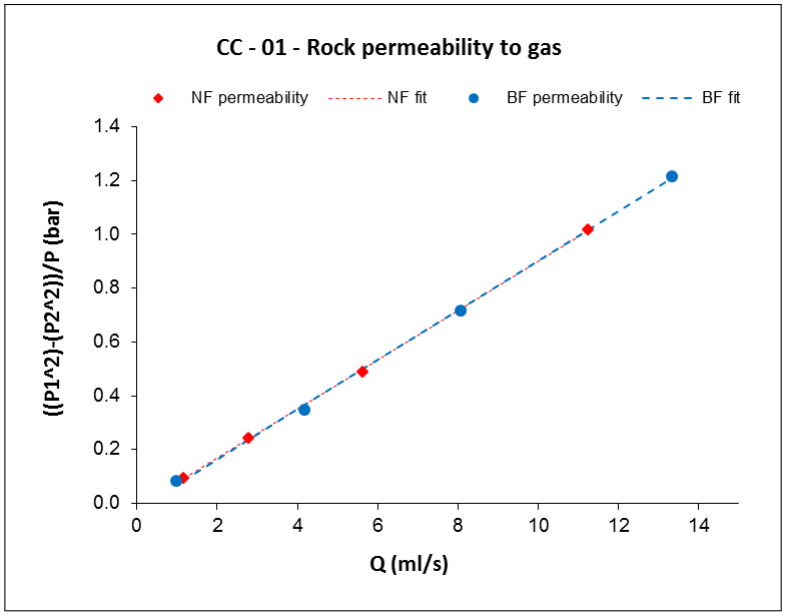

Figure 4.23: Relation between pressure drop and volumetric flow, at normal and back flow, for core number 1

Thus, the rock permeability results measured with gas, for core number 1, are presented in Table 4.15.

Core	Normal flow	Reverse Flow
1	241.4	239.3

Table 4.15: Rock permeability in mD for core number 1, measured with gas

4.2.2.2 CC-02

Similar to the procedure of core number 1, the rock permeability to gases was measured for core number 2, applying the equation 4.9, after measuring the pressure produced in the core at different flow rates.

For the calculations of core number 2, μ is 0.01777 cP; L is 7.392 cm; S is 11.39 cm^2, since the core diameter is 3.808 cm; P and P_2 are the atmospheric pressure, 1.013 *bar*; P_1 varies in accordance with the DP; and Q varies in accordance with the gas volume and time.

The relation between $(P_1^2 - P_2^2)/P$ and the flow rate (Q), for this core, is presented in Fig. 4.24.

Thus, the rock permeability results measured with gas, for core number 2, are presented in Table 4.16

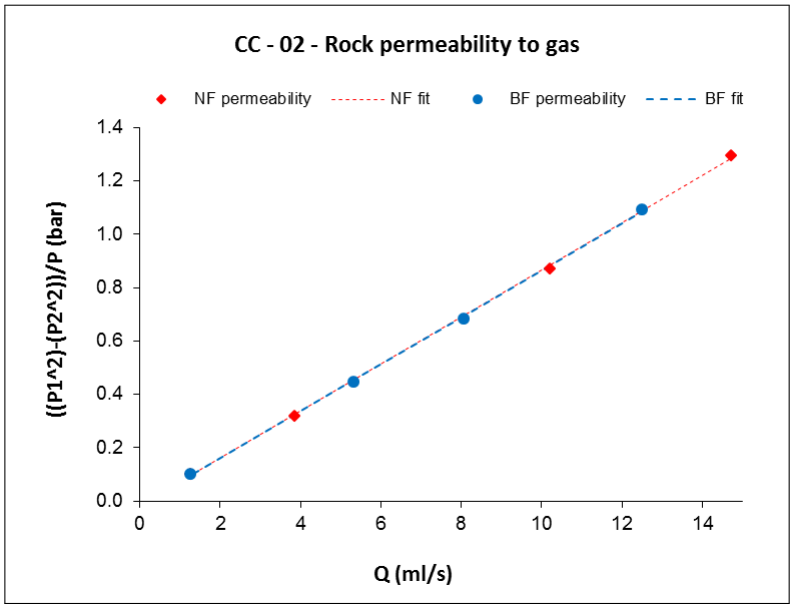

Figure 4.24: Relation between pressure drop and volumetric flow, at normal and back flow, for core number 2

Core	Normal flow	Reverse Flow
2	264.3	264.6

Table 4.16: Rock permeability in mD for core number 2, measured with gas

4.2.2.3 CC-03

Similar to previous core the rock permeability to gases was measured for core number 3, using nitrogen, and the same procedure. The rock permeability to gases was measured in normal and reverse flow, at 20 *bar* of confining pressure.

The permeability was estimated using equation 4.9, after measuring the pressure produced in the core at different flow rates.

For the calculations of core number 3, μ is 0.01777 cP; L is 7.381 cm; S is 11.38 cm^2, since the core diameter is 3.807 cm; P and P_2 are the atmospheric pressure, 1.013 *bar*; P_1 varies in accordance with the DP; and Q varies in accordance with the gas volume and time.

Thus, the rock permeability results measured with gas, for core number 3, are presented in Table 4.17

Core	Normal flow	Reverse Flow
3	263.75	275.23

Table 4.17: Rock permeability in mD for core number 3, measured with gas

4.2.2.4 CC-04

Similar to previous core the gas permeability was measured to core number 4.

The permeability was estimated using the equation 4.9, after measuring the pressure produced in the core at different flow rates.

For the calculations of core number 4, μ is 0.01777 cP; L is 7.366 cm; S is 11.39 cm^2, since the core diameter is 3.808 cm; P and P_2 are the atmospheric pressure, 1.013 *bar*; P_1 varies in accordance with the DP; and Q varies in accordance with the gas volume and time.

Thus, the rock permeability results measured with gas, for core number 4, are presented in Table 4.18

Core	Normal flow	Reverse Flow
4	211.36	208.44

Table 4.18: Rock permeability in mD for core number 4, measured with gas

4.2.3 Pore Volume measurement

The pore volume can be measured using two different procedures.

In first, the pore volume is measured in bulk, calculating the difference between the core weight when it is saturated with degassed formation brine and the core weight when it is completely dried. This value corresponds to the water that has gone into the core.

In second, the pore volume is measured by dynamic PV, which is measured through a tracer (naphthalene disulfonic), that is placed in the water injected in the core. Using online UV detectors, it is possible to know the time necessary for the tracer to travel through the entire core. Thus, knowing the flow rate applied and the time mentioned above, the pore volume can be calculated.

To do this measurement, the core was placed in a coreholder and saturated with water. Four different flow rates were used, 6 *ml/hr*, 12 *ml/hr*, 25 *ml/hr* and 50 *ml/hr*, and for each one the procedure was repeated two times.

To calculate, the pore volume value it is necessary to monitor the values recorded by the UV detector, convert them to absorbance and then normalize the values.

Therefore, knowing the specific time when the tracer is injected and when the peak of tracer takes place, it is possible to calculate the delay, which is the time between the moment when the tracer is injected until the moment when it comes out of the core. Once, the flow rate is known, as well as the delay, the volume can be calculated, multiplying the flow rate and the delay. Then, subtracting the dead volume (volume external to the core) we obtained the effective volume, in other words, the pore volume.

4.2.3.1 CC-01

After measuring the rock permeability to gases, the core is removed from the coreholder to measure the PV. In this case, for core number 1 the pore volume was measured in bulk. The result of the pore volume for core number 1 is 15.9 ml and the bulk porosity is 20.02%.

4.2.3.2 CC-02

For core number 2 the pore volume was measured both in bulk, and through a tracer (naphthalene disulfonic) using online UV detectors.

To do this measurement four different flow rates were used, 6 *ml/hr*, 12 *ml/hr*, 25 *ml/hr* and 50 *ml/hr*, and for each one the procedure was repeated two times.

In Fig. 4.25 it is presented a graph where four peaks are shown, one for each flow rate. It is possible to see that the four peaks have similar shape and the maximum of absorbance is between 16 *ml* and 18 *ml* of effective volume.

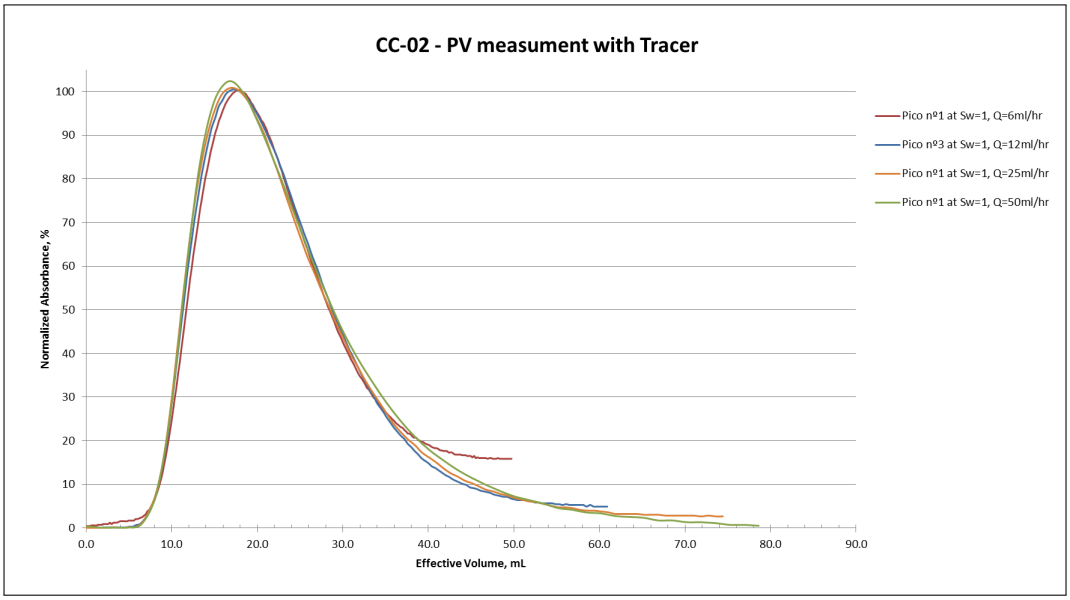

Figure 4.25: Pore volume measurement with tracer, for core number 2

The results of pore volume for core number 2 are shown in Table 4.19.

Usually, the value of dynamic PV is smaller that the value of PV measured in bulk, because when it is measured with a tracer the water is passing through the core just in one direction, while in bulk measurement, water saturates from all directions. In this case, for both methods the values of PV are very similar, however to be consistent to the other cores the value to be used is the value of PV in bulk. The value of bulk porosity was 20.07%.

	Q (*ml/hr*)	PV (*ml*)
in bulk	0	16.9
dynamic	6	17.81
dynamic	12	17.82
dynamic	25	16.87
dynamic	50	16.31

Table 4.19: PV measurement for core number 2

4.2.3.3 CC-03

The pore volume of core number 3 was measured in bulk and the result was 17.1 *ml* of pore volume, which corresponds to a 20.35 % of bulk porosity.

4.2.3.4 CC-04

The pore volume of core number 4 was measured in bulk and the result was 16.6 *ml* of pore volume, which corresponds to a 19.79 % of bulk porosity.

After the rock permeability measurement, the core is removed from the coreholder to measure the PV. In this case, the procedure was measured in bulk, calculated by the difference between the core weight when it is saturated with degassed formation brine, and the core weight when it is completely dried. The pore volume for core number 4 is 16.6 *ml*, and bulk porosity is 19.79%.

4.2.4 Measurement of rock permeability to water

After the pore volume measurement, the saturated core is placed back in the coreholder to measure the rock permeability to water.

The permeability is measured both in normal and back flow conditions using formation brine, with 30 *bar* of confining pressure, at 24 °C (viscosity = 1.183 *mPa.s* or *cP*) and at 120 °C (viscosity = 0.333 *mPa.s* or *cP*). For each experiment the DP was monitored for four flow rates, 10 *ml/hr*, 20 *ml/hr*, 30 *ml/hr* and 50 *ml/hr*, injected using an ISCO pump. The DP value is taken when the values are stable.

To measure the permeability at 120 °C the four coreholders were placed inside the oven at reservoir temperature, as shown in Fig. 4.26.

Moreover, to evaluate the DP behaviour at different flow rates, for normal and back flow, a graph was made, where the two lines were compared, for quality control of the measurement. Then, if the two lines were very different the measurement should be repeated.

To measure the rock permeability using brine the DP was measured in the core, for different flow rates

Figure 4.26: Coreholders inside the oven

and different temperatures. The Darcy equation, equation 4.10, has been applied to calculate the permeability.

$$\kappa(mDarcy) = \frac{\mu(cP) \times L(cm)}{S(cm^2)} \times \frac{Q(cc/h)}{\Delta P(bar)} \times 1013 \tag{4.10}$$

$Where\ :\ \kappa - permeability; \mu - fluid\ viscosity; L - Lenght\ of\ the\ core; S - area\ of\ the\ core; Q - flow\ rate;\ and\ \Delta P(bar) - pressure\ gradient\ across\ the\ core.$

4.2.4.1 CC-01

For the calculations at ambient temperature of core number 1, the parameters used were: μ is 1.183 cP; L is 6.977 *cm*; S is 11.38 cm^2, since the core diameter is 3.807 *cm*; Q is chosen; and the ΔP varies.

The graph that shows the relation between DP and flow rate, at ambient and reservoir temperature, is presented in Fig. 4.27.

At reservoir temperature, the same equation was used, (equation 4.10), however for the calculations, the values used were: μ is 0.333 *cP*; L is 6.977 *cm*; S is 11.38 cm^2, since the core diameter is 3.807 *cm*; Q is chosen; and the ΔP varies.

Thus, the rock permeability values measured with water are presented in Table 4.20.

	$K_w(mD)$, 24 °C		$K_w(mD)$, 120 °C	
Core	Normal Flow	Reverse Flow	Normal Flow	Reverse Flow
1	240.3	278.8	223.9	218.6

Table 4.20: Rock permeability in *mD* for core number 1, measured using water

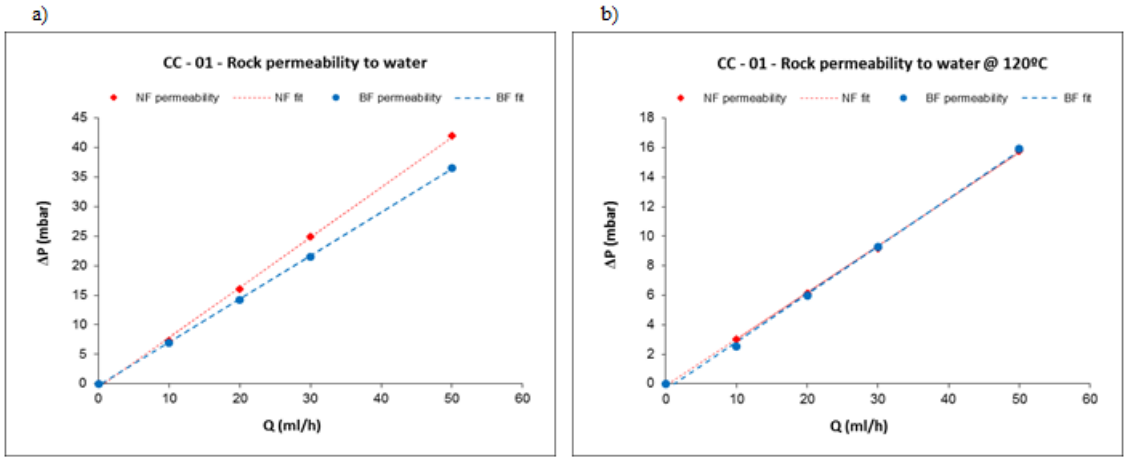

Figure 4.27: (a) Relation between DP and flow rate at ambient temperature and (b) Relation between DP and flow rate at 120 °C, for core number 1, back and normal flow

4.2.4.2 CC-02

For the calculations at ambient temperature, the parameters used were: μ is 1.183 cP; L is 7.392 cm; S is 11.39 cm^2, once the core diameter is 3.808 cm; Q is chosen and the ΔP varies.

The graph that shows the relation between DP and flow rate, at ambient and reservoir temperature, is presented in Fig. 4.28.

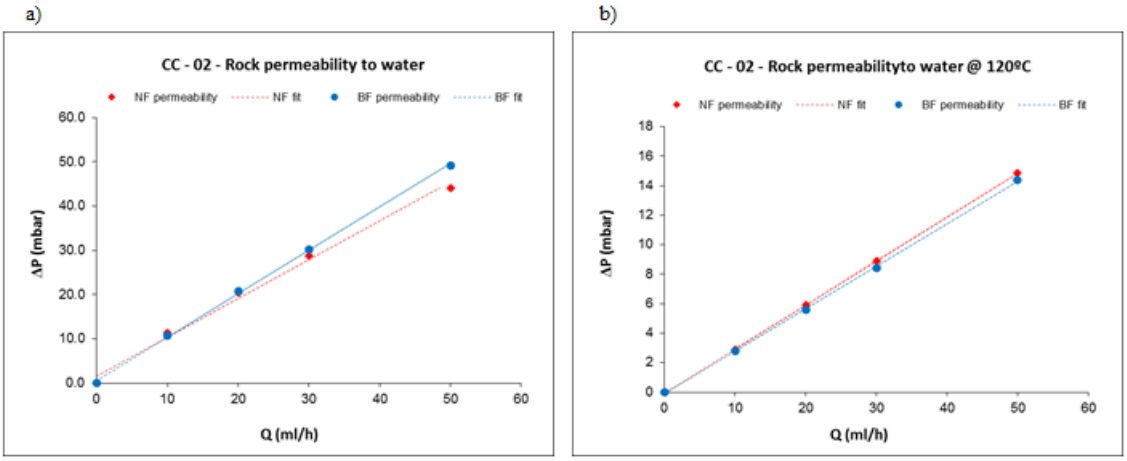

Figure 4.28: (a) Relation between DP and flow rate at ambient temperature and (b) Relation between DP and flow rate at 120 °C (right), for core number 2, back and normal flow

At reservoir temperature, the same equation was used, (equation 4.10), however for the calculations, the parameters used were: μ is 0.333 cP; L is 7.392 cm; S is 11.39 cm^2, once the core diameter is 3.808 cm; Q is chosen and the ΔP varies.

Thus, the rock permeability values measured with water are presented in Table 4.21.

	$K_w(mD)$, 24 °C		$K_w(mD)$, 120 °C	
Core	Normal Flow	Reverse Flow	Normal Flow	Reverse Flow
2	246.61	220.46	252.25	260.94

Table 4.21: Rock permeability in *mD* for core number 2, measured using water

4.2.4.3 CC-03

For the calculations at ambient temperature, the parameters used were: μ is 1.183 cP; L is 7.381 cm; S is 11.38 cm^2, once the core diameter is 3.807 cm; Q is chosen and the ΔP varies.

To measure the permeability at 120 °C, the same equation was used, (equation 4.10), however for the calculations, the parameters used were: μ is 0.333 *cP*; L is 7.381 *cm*; S is 11.38 cm^2, once the core diameter is 3.807 *cm*; Q is chosen and the ΔP varies.

Thus, the rock permeability values measured with water are presented in Table 4.22.

	$K_w(mD)$, 24 °C		$K_w(mD)$, 120 °C	
Core	Normal Flow	Reverse Flow	Normal Flow	Reverse Flow
3	258.51	260.77	221.06	215.82

Table 4.22: Rock permeability in *mD* for core number 3, measured using water

4.2.4.4 CC-04

For the calculations at ambient temperature, the parameters used were: μ is 1.183 cP; L is 7.366 cm; S is 11.39 cm^2, once the core diameter is 3.808 cm; Q is chosen and the ΔP varies.

To measure the permeability at 120 °C, the same equation was used, (equation 4.10), however for the calculations, the parameters used were: μ is 0.333 cP; L is 7.366 cm; S is 11.39 cm^2, once the core diameter is 3.808 cm; Q is chosen and the ΔP varies.

Thus, the rock permeability values measured with water are presented in Table 4.23.

	$K_w(mD)$, 24 °C		$K_w(mD)$, 120 °C	
Core	Normal Flow	Reverse Flow	Normal Flow	Reverse Flow
4	196.07	149.85	153.92	153.14

Table 4.23: Rock permeability in *mD* for core number 4, measured using water

4.2.5 Oil saturation

The next step is to measure the oil saturation. For this, it is necessary to remove the water, saturate the core with oil, and measure irreducible water saturation (Swi).

In the beginning of this procedure the core is 100 % saturated with brine, and is placed in contact with a ceramic disc that is permeable to brine, but not to oil. Thus, when the pressure is applied to the oil and to the brine, it forces the brine out of the core, through the ceramic disc. The saturation is finished when no more water comes out of the core.

The procedure is performed at ambient temperature and different pressure steps are applied: ambient pressure, 0.5 *bar*, 1 *bar*, 2 *bar*, 4 *bar*, 6 *bar*, 8 *bar* and the last step 10 *bar* (the maximum oil pressure limit allowed). In each step an amount of water is produced, and the volume of water is measured in a burette placed in the coreholder outlet. The burette reading is made twice a day. Once the water produced value is known, the water saturation value can be calculated, as well as the oil saturation value.

4.2.5.1 CC-01

The evolution of water saturation according to the pressure steps implemented and the time in days are presented in Fig. 4.29.

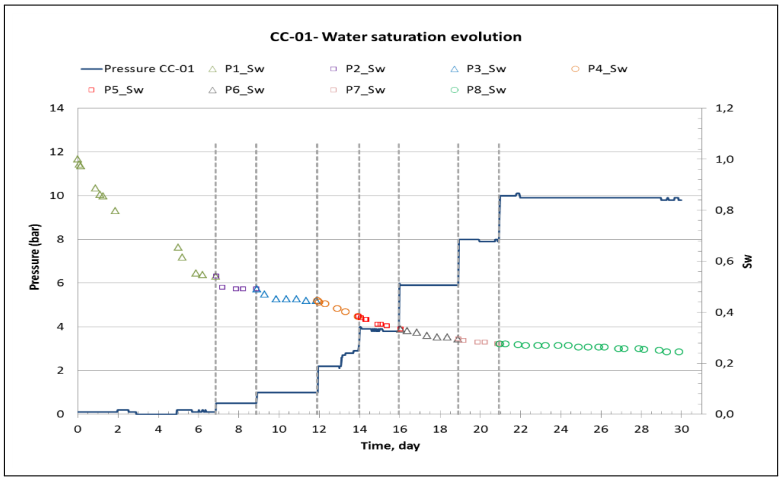

Figure 4.29: Water saturation evolution for core CC-01

With the information available it is also possible to draw a graph that shows capillary pressure evolution, Fig. 4.30. Thus, the value of Swi was 0.245 (24.5%).

Analysing the shape of the capillary pressure curve, it might be induced that the oil invade quickly the largest pores at first, and then the smallest pores. Therefore, the water saturation evolution decrease

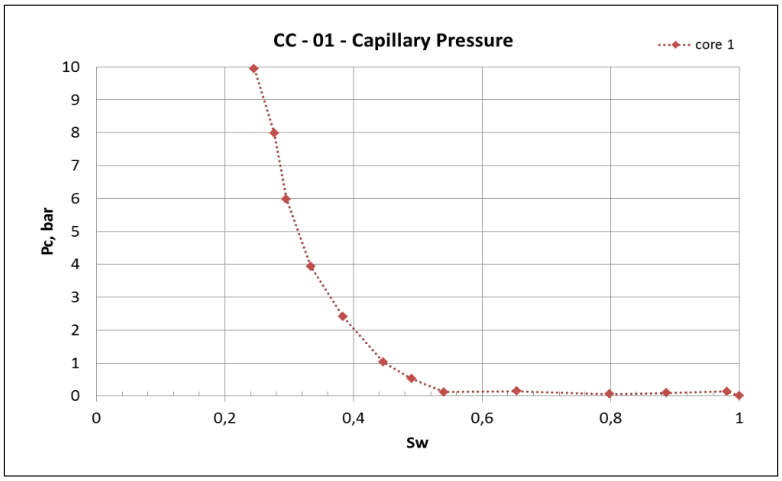

Figure 4.30: Capillary pressure evolution for core CC-01

fast, which means that the value of oil saturation increases fast during the first days.

The purpose to use the porous plate is to reach a low irreducible water saturation, and in this case the goal has been achieved.

4.2.5.2 CC-02

For core number 2, the evolution of water saturation according to the pressure steps implemented and the time in days, are presented in Fig. 4.31.

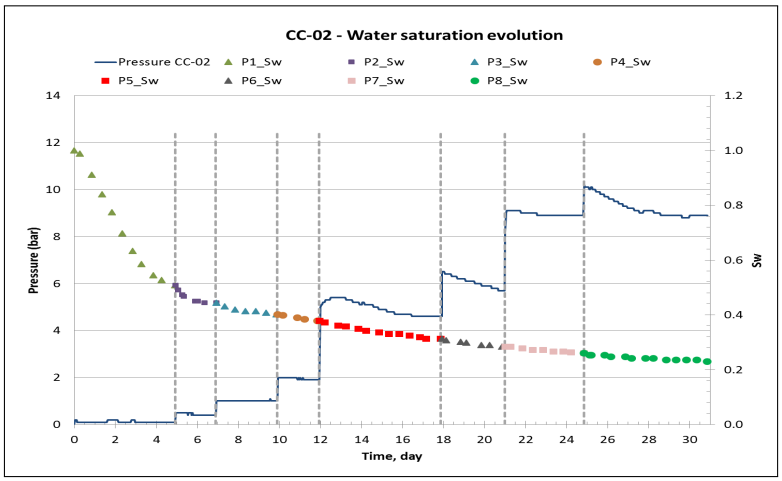

Figure 4.31: Water saturation evolution for core number 2

Similar to core number 1, the duration of oil saturation step was around 31 days, however some pressure steps had different duration, since the water production was not constant. It is possible to see that the value of pressure during the pressure step is not constant possibles due to a leak.

Fig. 4.32 shows the capillary pressure evolution of core number 1 and core number 2. The value of Swi is 0.231 (23.1 %).

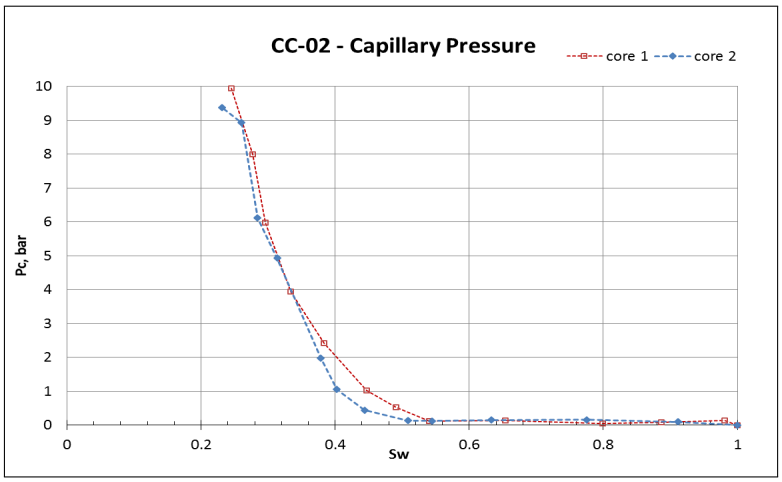

Figure 4.32: Capillary pressure evolution for core number 2 and for core number 1

Analysing the shape of the capillary pressure curve, it might be induced that the oil invade quickly the largest pores at first, and then the smallest pores. Therefore, the water saturation evolution decrease fast, which means that the value of oil saturation increases fast during the first days. For both cores, the curve shape is similar, however in core number 2 the curve grows slower, this effect can be due to the pressure drop and the duration of the pressure steps, or due to core characteristics.

The purpose to use the porous plate has been achieved.

4.2.5.3 CC-03

The evolution of water saturation of core number 3 is presented in Fig. 4.33 and capillary pressure evolution is shown in Fig. 4.34. Thus, the value of Swi is 0.189 (18.9%).

Analysing the shape of the capillary pressure curve, the water saturation evolution decrease fast. The curve shape for core number 3 is different that for core number 2 and 1, this effect can be due the pressure steps duration are different, in this case the pressure was increased only when the value of water in the burette was constant during three or four readings, or due to core characteristics. This way, the method was more efficient, since the value of Swi is lower.

The purpose to use the porous plate has been achieved.

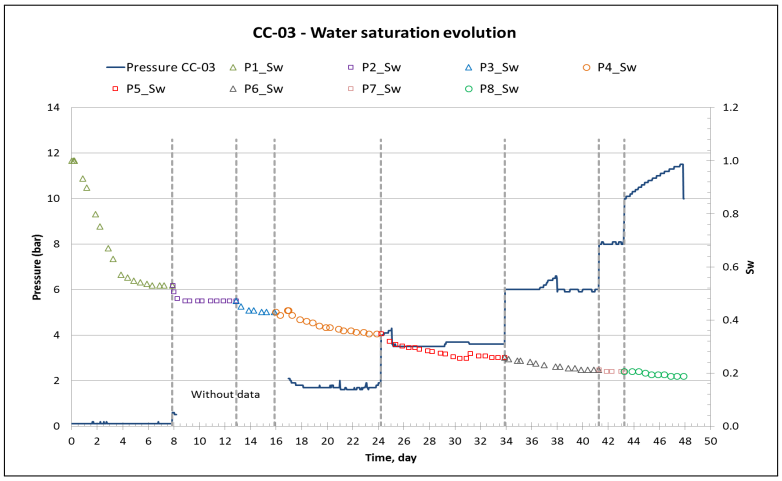

Figure 4.33: Water saturation evolution for core CC-03

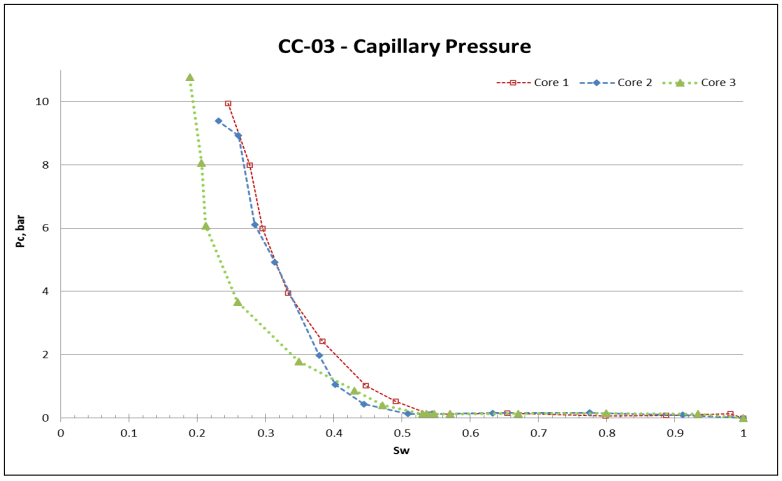

Figure 4.34: Capillary pressure evolution for core CC-03

4.2.5.4 CC-04

The evolution of water saturation of core number 4 is presented in Fig. 4.35 and capillary pressure evolution is shown in Fig. 4.36. Thus, the value of Swi is 0.130 (13.0%).

Analysing the shape of the capillary pressure curve, the water saturation evolution decrease fast. The curve shape for core number 4 is similar to core number 3, this effect can be due the pressure steps duration were similar (the pressure was increased only when the value of water in the burette was constant during three or four readings), or core characteristics between both core are similar. However, CC-04 was kept at oil saturation during more days than CC-03, namely at pressure step 10 *bar*.

The purpose to use the porous plate has been achieved.

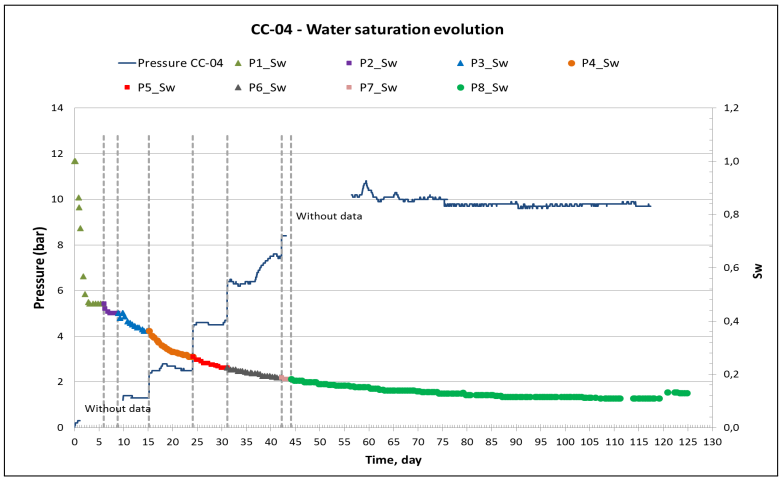

Figure 4.35: Water saturation evolution for core CC-04

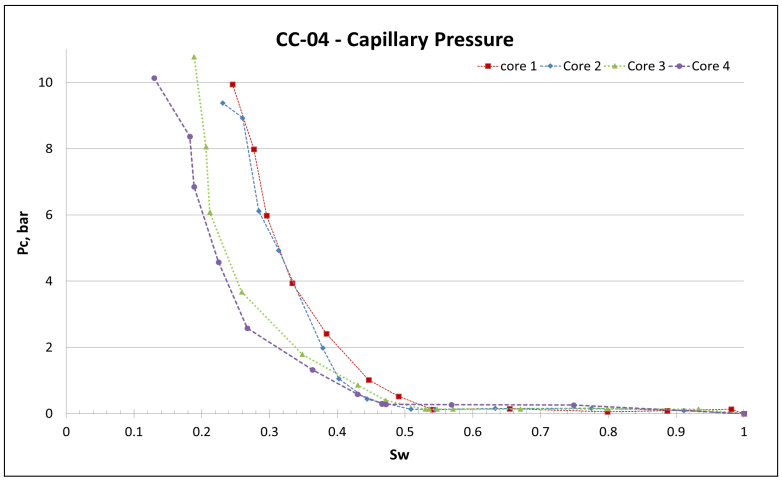

Figure 4.36: Capillary pressure evolution for core CC-04

4.2.6 Ageing

Once the core is saturated with oil until irreducible water saturation, the coreholder is placed in the ageing unit, where the core is aged at reservoir temperature and injected with oil, in order to measure the rock permeability to oil.

The purpose of this procedure is to make fluids adhere to the rock and restore the real wettability present in the field. For this, the time of ageing should be, at least, two weeks. During the ageing time the core is kept inside the oven at reservoir temperature, with confining pressure of 40 *bar* and pore pressure of 10 *bar*.

Relative rock permeability to oil is measured by injecting oil into the core, at different flow rates. In this case at 2 *ml/hr*, at 10 *ml/hr*, at 25 *ml/hr*, at 50 *ml/hr*, and at 100 *ml/hr*. The relative rock permeability

to oil is measured approximately once a week, after each measurement, the valves are closed and the core is aged again.

Only core number 1, 2 and 3 were submitted to ageing.

4.2.6.1 CC-01

The values of relative rock permeability to oil for core number 1, measured each week, are presented in Fig. 4.37.

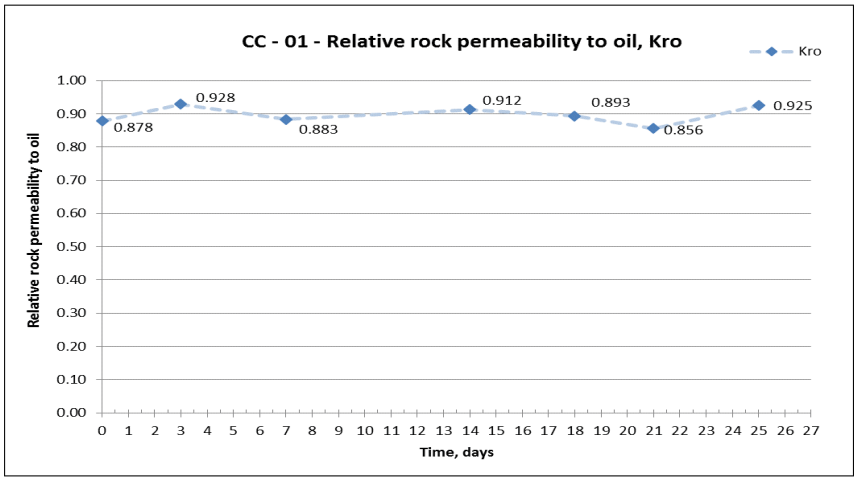

Figure 4.37: Relative rock permeability to oil, for core number 1

The ageing time for core number one was around 3 weeks and a half. Analysing Fig. 4.37, it is possible to conclude that during this time the value of Kro is approximately constant.

In the end of this procedure, once the core has all the initial reservoir conditions, it is ready to start the injection of brines with different salinity.

4.2.6.2 CC-02

The values of relative rock permeability to oil for core number 2, measured each week, are presented in Fig. 4.38.

The ageing time for core number 2 was around 2 months and a half, around two times more than core number 1, with the aim to investigate the impact of ageing duration in wettability. Analysing Fig. 4.38, it is possible to conclude that during this time the value of Kro was not constant like for core number 1, however at day 25, the Kro value was similar to CC-01, 0.899 and 0.92, respectively.

After this point, at day 32, the curve had a big drop, possible due to core wettability change and the oil has more difficulties passing through the core. However, due to this results the relative rock permeability

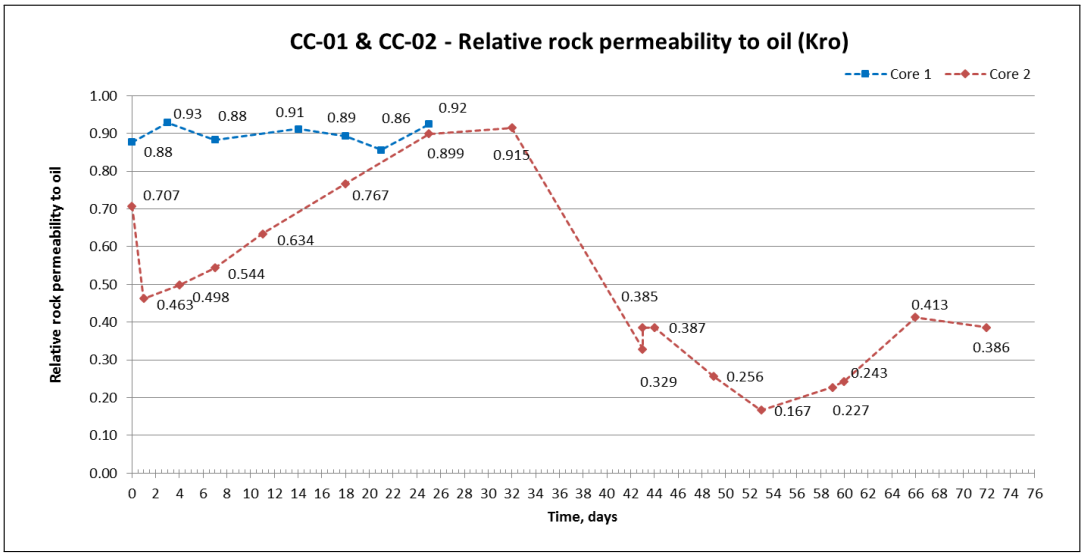

Figure 4.38: Relative rock permeability to oil, for core number 2 and 1

to oil was measured twice at the same day (day 43), and in the day after (day 44), the results were similar.

In the end of this procedure, once the core has reached all the initial reservoir conditions, it is ready to start the injection of brines with different salinities.

4.2.6.3 CC-03

The values of relative rock permeability to oil for core number 3, measured each week, are presented in Fig. 4.39.

The ageing time for core number 3 was around 2 months and a half, similar to core number 2. Analysing Fig. 4.39, it is possible to conclude that during this time the value of Kro was not constant like for core number 1, and the curve for core number 3 is very irregular. However, comparing the first and last values, there is a decrease, perhaps due to wettability change.

In the end of this procedure, once the core has reached all the initial reservoir conditions, it is ready to start the injection of brines with different salinities.

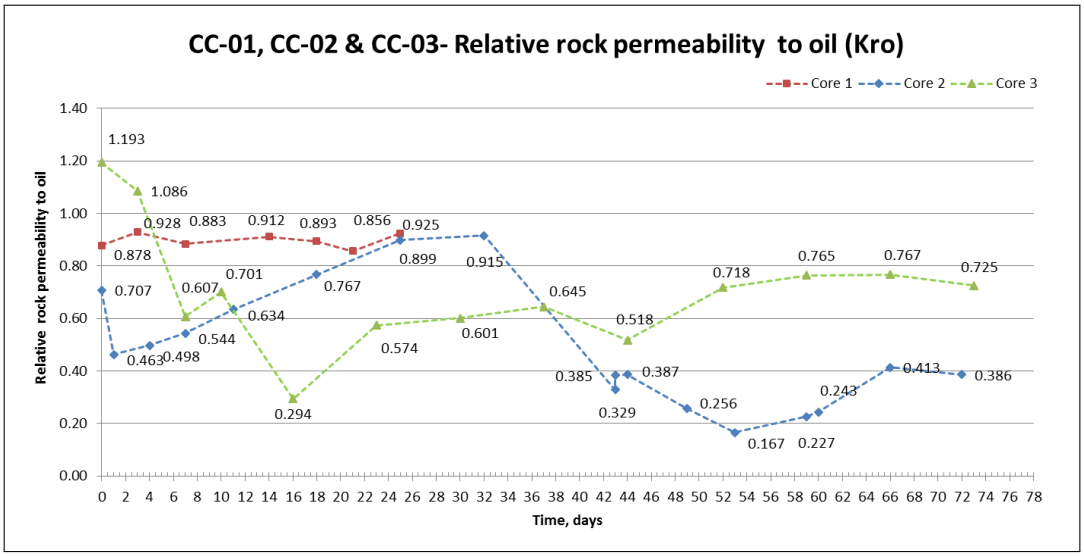

Figure 4.39: Relative rock permeability to oil, for core number 3, 2 and 1

4.3 Core flooding methodology

4.3.1 Unit

In the core flooding unit, the coreholder and respective core is placed inside an oven. During the experiment, the overburden pressure is kept at 40 *bar* and the pore pressure 10 *bar*.

The coreholder has one inlet and two outlets. The inlet is connected to a pump that injects the fluids, and the inlet pressure is measured in this connection. One outlet is connected to a conductivity cell that monitors the conductivity of the fluids coming out from the core, which is then connected to a BPR and a high pressure burette, Fig. 4.40, or a sample collector, Fig. 4.41.The other outlet is used to measure the outlet pressure.

A pump is used to control the inlet pressure and the flow rate, and thus change it easily.

In Fig. 4.40, the burette is full with formation brine and connected with a tube to the coreholder outlet. Thus, the oil produced comes out from the core, travels thought the tube, and goes to the burette. As the oil is less dense than water, it floats on the top, where the volume can be measured and monitored.

In Fig. 4.41, the sample collector is placed after a BRP to keep the back pressure. The oil produced travels through the tube, to the BPR and is collected in test tubes placed in the sample collector. Thus, the test tube has water and oil, and the oil volume can be quantified by visual inspection. However, this technique is not very accurate and another technique is used, where the water is removed with a syringe, and dichloromethane is added to clean the tube, after evaporation, the material is weighted and the oil quantified.

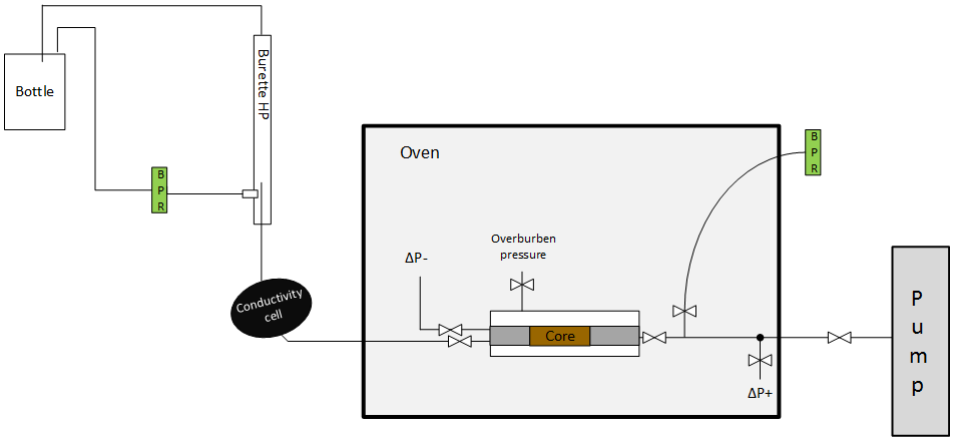

Figure 4.40: Core flooding unit using high pressure burette

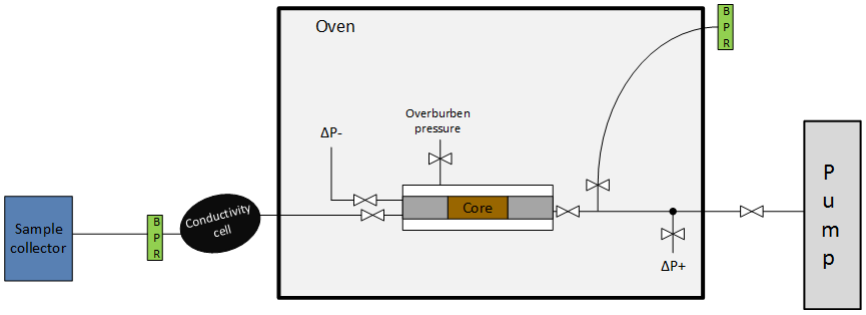

Figure 4.41: Core flooding unit using sample collector

4.3.2 Methodology

Before performing a core flooding some calculations need to be made, for each core and for each case. It is important to know the volume of oil present in a core, that corresponds to the maximum of volume that can be produced.

Therefore, since the pore volume and irreducible water saturation are known, it is possible to know the oil saturation and consequently the oil and water volume present in the core.

The oil saturation, So, is given subtracting the Swi to 1. And the volume of oil present in the core, was calculated applying equation 4.11.

$$Volume\ of\ oil\ (ml) = PV \times So \tag{4.11}$$

$Where: PV - pore\ volume\ (ml)\ and\ So - Oil\ saturation$

A different sequence of brines were injected in each core. Here, it will be only described the core flooding procedure for CC-01 and CC-02. The first injection was always formation brine, that was used

as a reference in terms of oil recovery. Afterwards SSW was injected, SSW is easily available in the field and the salinity is around 5 times lower than FB, and after SSW, the brine injected varies according to the core used.

It is important to monitor pressure and conductivity during all the experiment. The conductivity, is variable with salinity and both variables are directly proportional. This means that when salinity increases, the conductivity increases and when salinity decreases, conductivity decreases. Thus, it is expected that during FB injection the values of conductivity is high and decreases with the following injections. It is also expected that when oil passes through conductivity cell, the conductivity value is zero.

The DP should increase in same proportion that the flow rate increases, which means that if the flow rate increase four times, for example since 3 *ml/hr* until 12 *ml/hr*, the value of DP should increase also four times. It is also expected that the values of DP decrease, when a brine with less salinity is injected, as a result of the lower viscosity. Generally low salinity brines have a lower viscosity than formation brine.

The oil recovery factor was calculated using the equation 4.12.

$$Oil\ recovery\ (\%) = \frac{V_{prod}}{OOIP} \times 100 \tag{4.12}$$

$Where: V_{prod} - Volume\ of\ oil\ produced\ (ml)\ and\ OOIP - Original\ oil\ in\ place\ (ml)$

4.4 Summary

To summarize the experimental methodology, the rock permeability results in *mD* are presented in Table 4.24, namely, rock permeability values measured with gas at normal and back flow and measured with water at ambient temperature and at reservoir temperature, normal and back flow.

	Normal Flow			Back Flow		
Core	K_{gas}, 24 °C	K_w, 24 °C	K_w, 120 °C	K_{gas}, 24 °C	K_w, 24 °C	K_w, 120 °C
1	241.4	240.3	224.2	239.3	278.8	218.9
2	264.3	246.6	252.2	264.6	220.5	260.9
3	263.7	258.5	221.3	275.2	260.8	216.1
4	211.4	196.1	154.1	208.4	149.8	153.3

Table 4.24: Cores permeability in *mD*

The results obtained for each core are not very heterogeneous, because there are no significant differences between the implemented methods.

After rock permeability measurement, all the cores were submitted to the same procedures: oil saturation and ageing. The results obtained are different, as shown in Fig. 4.36 and Fig. 4.39.

The graph that shows capillary pressure evolution is presented in Fig. 4.36. Analysing the shapes of capillary pressure curves, it is possible to conclude that the cores are all oil wet. The curve shape for core number 4 is similar to core number 3, because the pressure steps duration were similar. And the curve shape for core number 2 is similar to core number 1, because the pressure steps duration were also similar.

The values of relative rock permeability to oil are presented in Fig. 4.39. It is possible to conclude that the value of Kro was not constant for core number 3 and 2, however it is constant for core number 1. Thus, the curve for core number 3 and 2 is irregular and have a drop, this can indicate alteration of core wettability, since the oil had more difficulties in passing through the core.

Some of the differences are due to the parameters that changed, for example the number of days during oil saturation, and ageing. And some of the differences are due to core characteristics.

Chapter 5

Results and Discussion

The following chapter details the experiments' results and the respective discussion. The Chapter is organized as follow:

- **Section 5.1** presents the results of the core flooding performed over core CC-01.
- **Section 5.2** describes the results of the core flooding performed over core CC-02.
- **Section 5.3** summarises the chapter.

The impact of low salinity brine on oil recovery will be investigated, through core flooding experiments over CC-01 and CC-02. The formation brine was used in both core flooding, as a reference in terms of oil recovery. The Formation brine injection was followed by Synthetic Sea Water injection and finally a dilution of the SSW or a modified SSW. For each core, at least 3 brines were tested at two flow rates, 3 *ml/hr* and 12 *ml/h*.

During the experiment, oil production, pressure, conductivity, ions concentrations and pH were monitored.

5.1 CC-01

The first core flooding experiment was performed over core number 1. In this case, the pore volume is 15.9 *ml*, Swi is 0.245 and So is 0.755. The volume of water in the core is 3.9 *ml* and the volume of oil 12 *ml*, given by equation 4.11.

In this core four different brines were injected:

- First injection: FB

- Second injection: SSW
- Third injection: SSW 1/10
- Fourth injection: SSW 1/25

According to literature it is expected that SSW would change the core wettability, because the SSW is 5 times less salty than the formation brine, and also because the sulphate concentration in this brine is around 10 times greater than in the formation brine.

In Fig. 5.42 the oil recovery results for each brine are presented, as well as, the flow rate, the conductivity and DP results. In Fig. 5.43 are presented the oil recovery results, the DP values and the flow rate implemented. The oil recovery factor was calculated using the equation 4.12

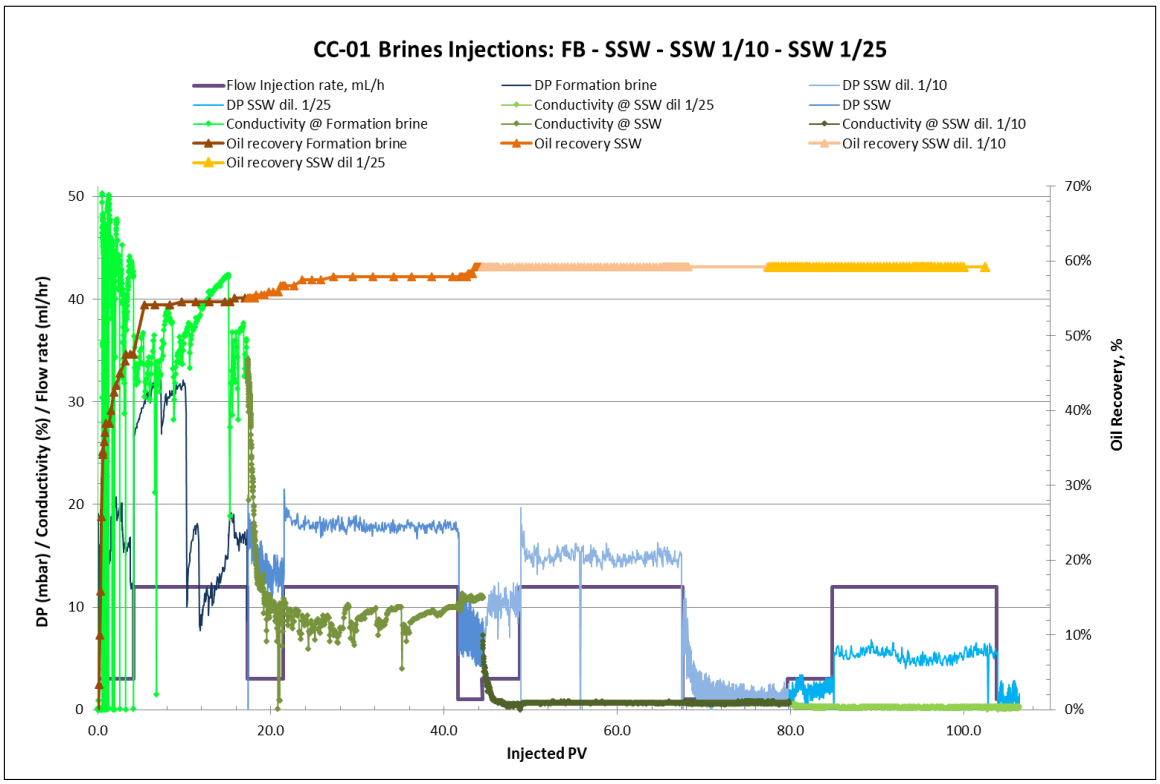

Figure 5.42: Brines injection results for core number 1

Formation brine was first injected at 3 *ml/hr* and then when the oil production was stable increased to 12 *ml/hr*.This injection produced 55 *%* of the original oil in place. 275 *ml* of FB were injected, which means 17.30 PV. During this injection the high salinity damaged the pump, which lead to irregular DP data and conductivity, however it is possible to see that during this injection the conductivity presents high values as a result of the high salinity level.

Later, injection was switched to SSW at 3 *ml/hr* and after 12 *ml/hr*. This injection showed extra 4.2 *%*

oil production, which is an indication of wettability alteration to less oil-wet. Additional 429 ml of SSW were injected which means 27 PV. It is possible to see that the conductivity for this brine is lower than for FB, due to low salinity. However in the first moments of SSW injection conductivity values were high, because FB is flowing out of the core. In this case, the DP is more stable than comparing with formation brine DP. After the oil production stopped, the flow rate was switched to 1 *ml/hr*, to keep the core in stand-by until next injection. During this time, no extra oil was produced, however the outlet was clean, and the oil trapped went out.

During the injection of both brines the high pressure burette was used. The oil produced was kept in the upper part and the oil volume was measured daily.

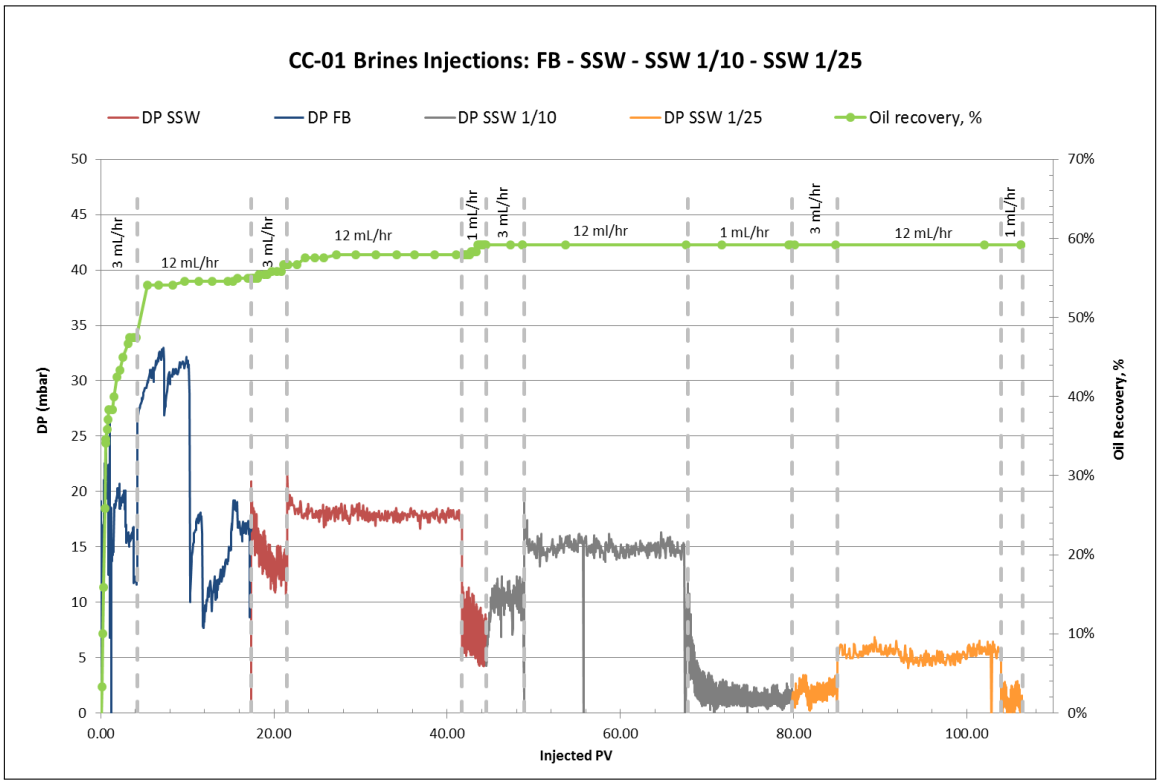

Figure 5.43: Brines injection results for core number 1

After the oil production by SSW stopped, SSW diluted 10 times was injected, to study if the injection of a brine with low salinity can give extra oil production, compared to previous brine. Similar to previous brines, the first flow rate was 3 *ml/hr* and then 12 *ml/hr*. The SSW 1/10 injection did not show any extra oil production, which means that this salinity was not capable to change the core wettability to less oil-wet. Additional 561 *ml* of SSW 1/10 were injected, which means 32 PV. It is possible to see that the conductivity for this brine is lower than for SSW, due to lower salinity. However in the first moments of SSW 1/10 injection conductivity values were high, because SSW and FB are flowing out of the core. The DP is stable and lower than for SSW. After the oil production stopped, the flow rate was switched to

1 *ml/hr*, to keep the core in stand-by until next injection.

The last injection was SSW 1/25, first at 3 *ml/hr* and then 12 *ml/hr*, with the objective to examine if this brine with low salinity, 1.7 *g/L*, can produce extra oil compared to the previous brines. With the SSW 1/25 injection no extra oil was produced, which means that this brine was not capable to change the core wettability to less oil-wet. Additional 423 *ml* of SSW 1/25 were injected, which means 26.6 PV. It is possible to see that the conductivity for this brine is lower than for SSW 1/10, due to lower salinity, however in the first moments of SSW 1/25 injection conductivity values were high because previous brines are flowing out of the core. The DP is stable and lower than for SSW 1/10. After the oil production stopped, the flow rate was switched to 1 *ml/hr*, to keep the core in stand-by until next step.

During the injection of both brines the sample collector was used, and the fluids produced were kept in test tubes. In this case just water was produced, however this water was kept to future analyses.

Thus, during the experiment 1689 ml of different brines were injected, which means 106.26 PV, leading to the production of 7.1 *ml* of oil, 59.17 *%* of the original oil in place (12 *ml*).

In the end of injections, the water kept in the test tubes was submitted to analyses, that allows a better understanding of what happens inside the core. Thus, the effluent ionic composition was analysed, namely, calcium, magnesium, potassium, chloride, sodium and sulphur. Main results for calcium and sulphur concentration are shown in Fig. 5.44 and Fig. 5.45, respectively. All other results are shown in appendix A.

In Fig. 5.44 it is possible to see the values of calcium (Ca^{2+}) in the effluent, as well as the level of calcium in both initial solutions, SSW 1/10 and SSW 1/25. Each dot in the plot corresponds to a sample analysed. No samples were analysed between 65 PV and 77 PV, because during this period of time the flow rate was 1 *ml/hr*.

Analysing the results of calcium (Ca^{2+}) composition, it is possible to see that the effluent values were above the level of initial solution. This may indicate the core dissolution or previous brines production. At the first moments it is possible to see high concentration of this ion, due to production of FB and SSW trapped inside the core and pushed by new brines. The rock dissolution can happen due to the lower calcium concentration present in the injected brine, which causes dissolution of the calcium carbonate from the rock and establishes equilibrium with the brine.

In Fig. 5.45, it is possible to see the values of sulphur (S) in the effluent, as well as the level of this ion in both initial solutions, SSW 1/10 and SSW 1/25.

Analysing the results of sulphur (S) composition, it is possible to see that the effluent values for SSW 1/25 were above the level of initial solution. This may indicate a very little presence of oil in the water, or when the water passed through the core saturated with oil, this action changed the brine composition.

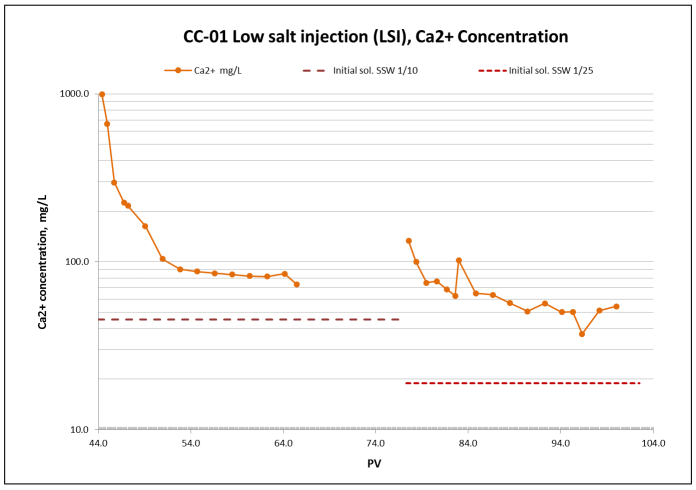

Figure 5.44: Results of analyses performed to the effluent to measure the Calcium concentration

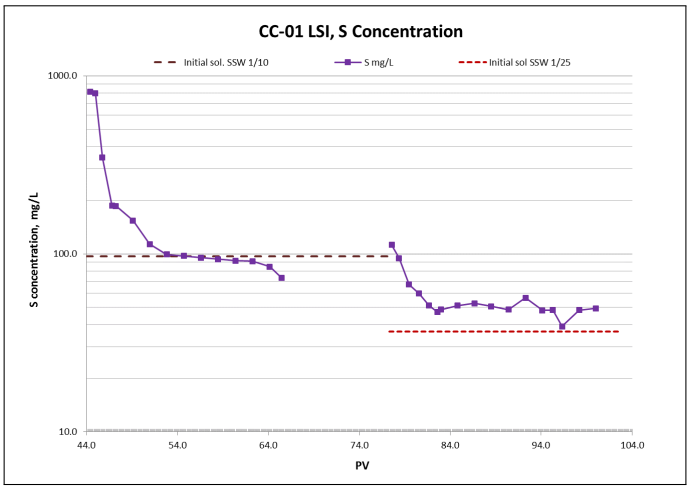

Figure 5.45: Results of analyses performed to the effluent to measure the Sulphur concentration

5.2 CC-02

The second core flooding experiment was performed over core number 2. In this case, the pore volume is 16.9 *ml*, Swi is 0.231 and So is 0.769, The volume of water in the core is 3.9 *ml* and the volume of oil 13 *ml*, given by equation 4.11.

In this core three different brines were injected:

- First injection: FB
- Second injection: SSW
- Third injection: SSW mod

Similar to core number 1, the first injection was formation brine, that was used as a reference in terms of oil recovery. After the FB, SSW was injected, since it is easy the access to this brine and the salinity is around 5 times lower than FB, and also to validate the set-up and results accuracy. Finally, SSW modified was injected.

According to literature is expected that SSW would change the core wettability, because the SSW is 5 times less salty than the formation brine, and also because the sulphate concentration in this brine is around 10 times greater than in formation brine. Is also expected that the injection of SSW mod mobilize oil, once this brine have 4 times more SO_4^{2-} than SSW, and less Na^{2+}.

In Fig. 5.46 are presented the oil recovery results for each brine, the flow rate, the conductivity and DP results also for each brine. Oil recovery factor was calculated using the equation 4.12.

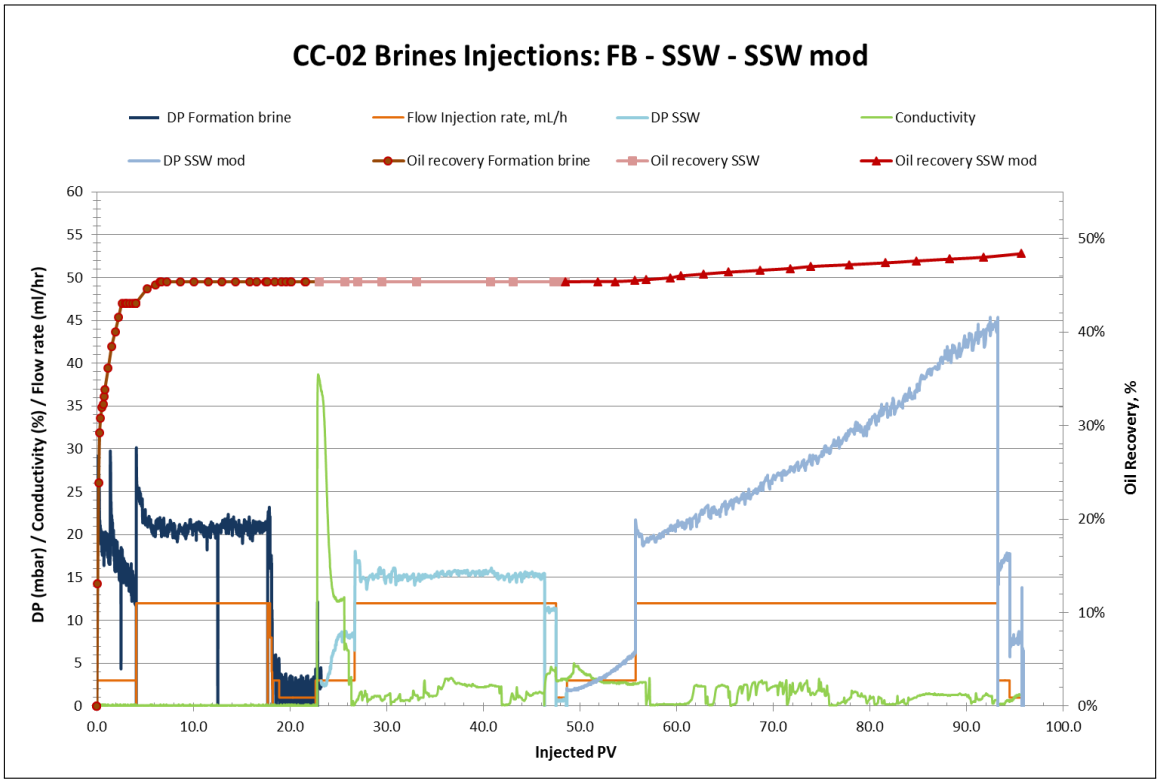

Figure 5.46: Brines injection results for core number 2

Formation brine was first injected at 3 *ml/hr*, then when the oil production was stable increased to 12 *ml/hr*, and in the end of production decreased to 1 *ml/hr*, to keep the core in stand-by until next injection. This first injection produced around 45.38 % of the original oil in place. 389.4 *ml* of FB were injected, which means 23.04 PV. During this injection the pump worked in normal conditions, and DP data is regular, however the conductivity cell presented problems and conductivity data was not available.

During the injection the high pressure burette was used. The oil produced was kept in the upper part

and the oil volume was measured daily.

Later, the injection was switched to SSW at 3 *ml/hr* and after 12 *ml/hr*, this injection did not showed extra oil production. Additional 430 *ml*of SSW were injected, which means 25.44 PV. It is possible to see that the conductivity for this brine is lower than for FB, however in the first moments of SSW injection, the conductivity values were high, because FB is flowing out of the core. After a long time injecting without oil production the flow rate was switched to 1 *ml/hr*, to keep the core in stand-by.

After SSW injection stopped, SSW modified was injected to study if the injection of a brine with same salinity, but different ionic composition can produce extra oil, compared to the previous brine. Similar to previous brines, the first flow rate was 3 *ml/hr* and then 12 *ml/hr*. The SSW mod injection showed extra 3 *%* oil production. However, the quantity was difficult to quantify, and to know the exact time and quantity produced. Thus, in Fig. 5.46 the line correspondent to SSW mod oil recovery is a approximation. This means that, maybe this ionic composition is capable to change the wettability. Additional 794 *ml* of SSW mod were injected, which means around 47 PV. It is possible to see that the conductivity for this brine is in the same level than for SSW, once both brines have the same salinity, with TDS around 42 *g/L*. The DP was not stable, once it increase since the first flow rate, this can indicate core damaged, or obstruction.

As explained before in a carbonate reservoir the rock surfaces have a positive charge while the acidic components of oil have a negative charge, causing the rock to be oil-wet or mixed-wet. If the active anions in the water, for example SO_4^{2-}, have a higher affinity to the rock surface than the acidic oil components, the anions are adsorbed and the oil is desorbed. This process explains the extra oil production with SSW mod.

During the injection of both brines the sample collector was used, and the fluids produced were kept in test tubes. In Fig. 5.47 are presented some of the test tubes collected from SSW mod injection, where it is possible to see some of the oil produced.

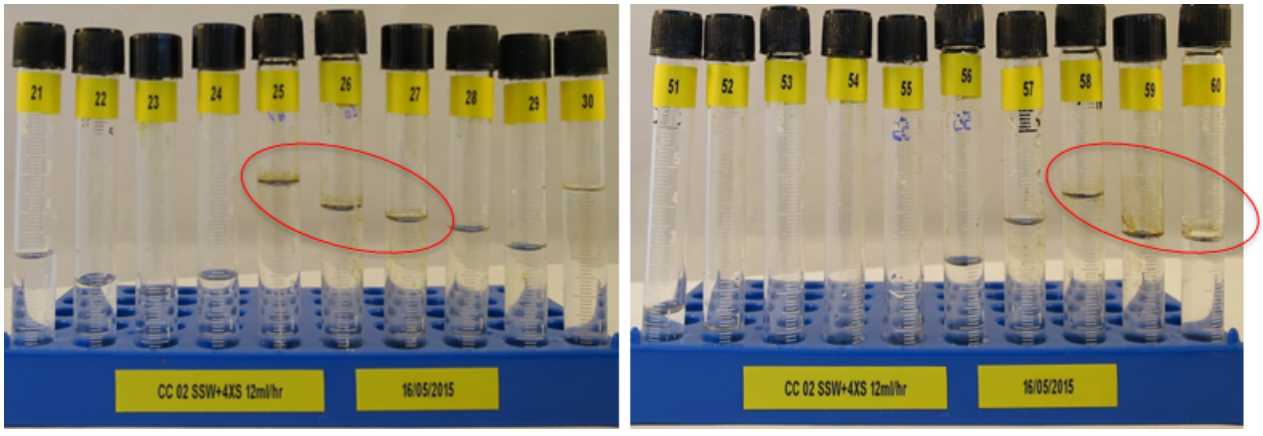

Figure 5.47: Test tubes from SSW mod injection through core number 2

Thus, during the experiment around 1617 *ml* of different brines were injected, which means 95.7 PV, leading to the production of 6.29 *ml* of oil, 48.38 % of the original oil in place (13 *ml*).

In the end of injections, similar to core number 1, the water kept in the test tubes was submitted to analyses, that allows a better understanding of what happens inside the core. Thus, the effluent ionic composition was analysed, namely, calcium, magnesium, potassium, chloride, sodium and sulphur for SSW injection and for SSW mod injection. Main results for calcium concentration are shown in Fig. 5.48. All other results are shown in appendix B. In these figures the level of ions produced is similar to the level of ions in initial solution.

In Fig. 5.48 it is possible to see the values of calcium (Ca^{2+}) in the SSW mod effluent, as well as the level of calcium for initial solutions, SSW at the beginning and then SSW mod. Each dot in the plot corresponds to a sample analysed.

Analysing the results of calcium (Ca^{2+}) composition it is possible to see that the effluent values were below the level of initial solution, the opposite of what happened to core number 1. Which means that in this case did not happen core dissolution, possibly because the brine injected was not a low salinity brine with no need to establish equilibrium with calcium carbonate from the rock. This difference between calcium concentration can indicate that some calcium precipitate.

In the beginning, it is possible to see that the calcium concentration is above the level of SSW initial solution, possible because FB production.

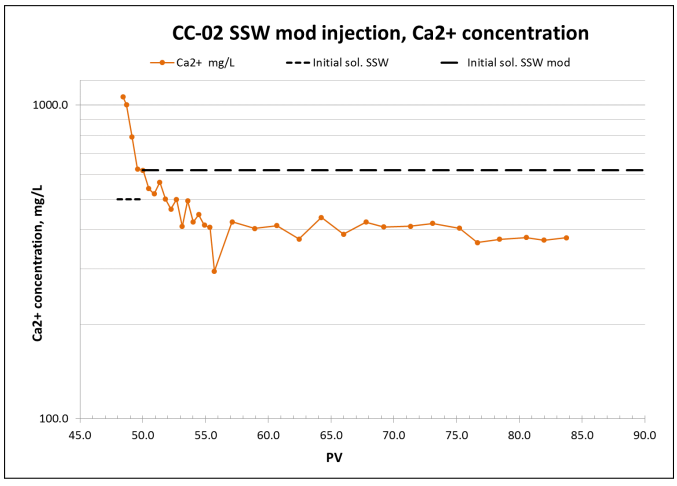

Figure 5.48: Results of analyses performed to SSW mod effluent to measure the Calcium concentration

5.3 Summary

In this section the results for the core flooding experiment over both cores are summarized and compared.

The main objective of the project was to modify the salinity and the ionic composition of SSW to improve the oil recovery in oil wet cores, in order to study the impact of low salinity and ionic composition on oil recovery from a carbonate reservoir.

The PV injected for each brine is present at Table 5.25.

Brine	Flow rate(*ml/h*)	PV injected in CC-01	PV injected in CC-02
FB	3	4.13	4.05
	12	13.18	13.61
Total		17.31	23.04
SSW	3	4.15	3.46
	12	20.18	20.85
Total		27.17	25.44
SSW 1/10	3	4.37	
	12	18.86	
Total		35.32	
SSW 1/25	3	5.17	
	12	18.94	
Total		26.60	
SSW mod	3		7.11
	12		37.48
Total			47.20

Table 5.25: Values of PV injected

Thus, in Table 5.25, it is possible to see the number of PV injected in each core, at 3 *ml/hr*, 12 *ml/hr* and the total, the sum of the PV injected at 3 *ml/hr*, at 12 *ml/hr* and if is the case at 1 *ml/hr*. During the experiment was attempted to inject the same value of PV in the different cores, in accordance to the brine. It is possible to see that for the common brines injected, FB and SSW, the values were similar, however the results were different.

It is present in Fig. 5.49 the results of common injections for core number 1 and core number 2. In this figure the oil recovery results, the DP and the flow rate are presented.

During the injection of FB at 3 *ml/hr*, core number 1 produced 47.5 % and after 12 *ml/hr*, produced 55 % of the OOIP and core number 2 produced 43.1 % at 3 *ml/hr* and after the injection at 12 *ml/hr*, produced 45.4 % of the OOIP. The difference of oil produced is around 10 %.

During the injection of SSW at 3 *ml/hr*, core number 1 produced 1.67 % and after 12 *ml/hr*, produced 4.2 % of the OOIP and for core number 2 no increased oil recovery was observed. The difference of oil produced is around 4.2 %.

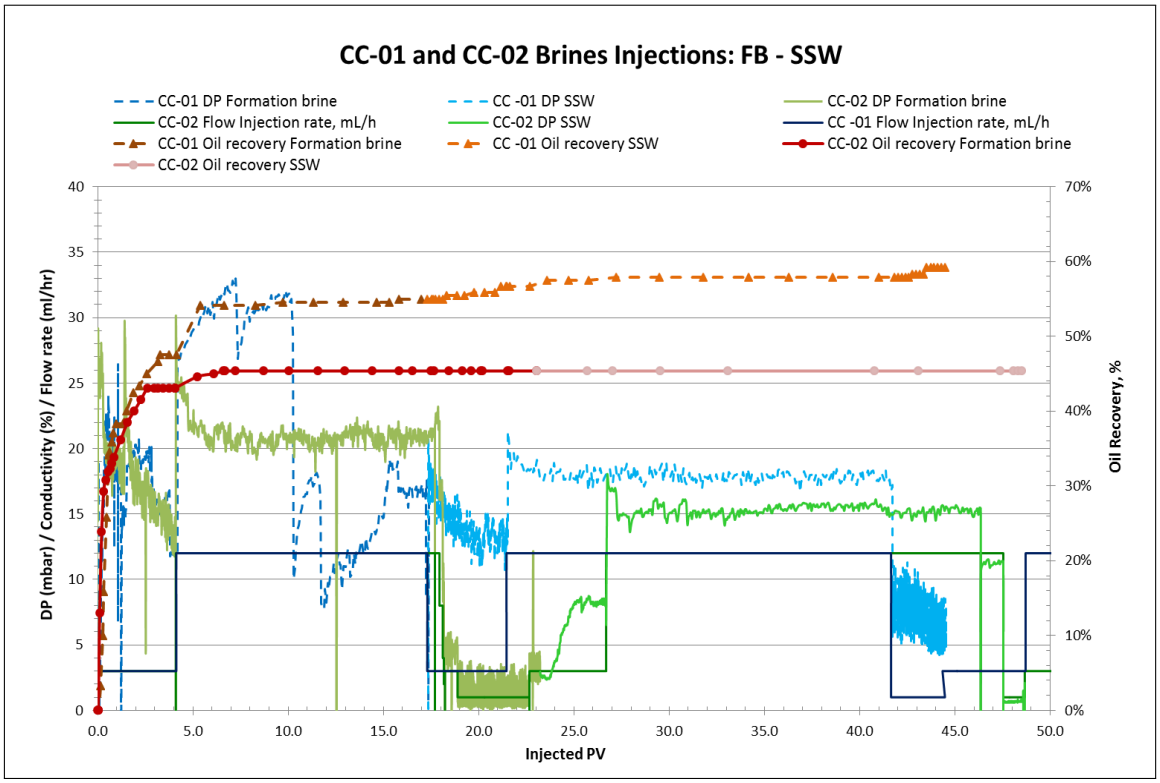

Figure 5.49: FB and SSW injection results for core number 1 and core number 2

In core number 1, no increased oil recovery was observed when injecting SSW diluted 10 times and 25 times, and in core number 2, when injecting SSW modified the oil recovery increased around 3 %.

Therefore, despite the preparation of the cores was equal, the conditions were not equal. The 10 % difference of oil recovery during FB injection may indicate that the core number 2 is more oil wet than core number 1, and that is more difficult to produce oil.

It is also important to emphasize that the injection of low salinity brine, SSW diluted, did not show extra oil production, however the injection of SSW modified with more concentration of SO_4^{2-} showed extra oil production. This means that not only the salinity is important, but also the ionic composition.

Chapter 6

Conclusion

The main objective of the experiment was to modify the salinity and the ionic composition of sea water to improve the oil recovery in oil wet cores. To achieve this goal four cores were prepared to perform core flooding, however in this work just two core flooding experiments are described, due to time frame.

The conclusion about this study can be briefly summarized as:

- The oil recovery by formation brine injection was 55 % of OOIP for core number 1, CC-01. At the first flow rate, 3 *ml/hr*, 47.5 % of OOIP was produced.
- In core number 1 when injected SSW the oil recovery increased 4.2 %. At the first flow rate, 3 *ml/hr*, 1.67 % of OOIP was produced.
- No increased oil recovery was observed when injecting SSW diluted 10 times and 25 times, in core number 1.
- The oil recovery by formation brine injection was 45.4 % of OOIP for core number 2, CC-02. At the first flow rate, 3 *ml/hr*, 43.1 % of OOIP was produced.
- No increased oil recovery was observing when injected SSW in core number 2.
- In core number 2, when injecting SSW modified the oil recovery increased around 3 %.

Despite the preparation of the cores was equal, the conditions were not equal. The 10 % difference of oil recovery during FB injection it might be because core number 2 is more oil wet than core number 1, and that is more difficult to produce oil or due to core characteristics that are different.

It is important to emphasize that the injection of low salinity brine, SSW diluted, did not show favourable results, however the injection of SSW modified with more concentration of SO_4^{2-} showed favourable results, this means that not only the salinity is important, but also the ionic composition.

This four experiments are not enough to keep or discard a process, it is important to perform more experiments with different brines, with different salinities and ionic composition.

6.1 Future Work

To improve the oil recovery it is suggested as future improvement, perform the crude oil saturation under reservoir temperature, to make the core more oil-wet. Another improvement can be, perform the ageing to all cores during the same time, to discard the hypothesis that one core is more oil-wet than another, due to ageing time.

To improve the oil recovery it is suggested as future work to inject a surfactant, Surface Active Agent. A surfactant can be injected to lower the Interfacial tension (IFT) or capillary pressure that do not allow the oil to move through the core, and be produced. Oil recovery improvement occurs by reducing both IFT and capillary forces in the formation.

Surface active agents are usually organic compounds with a chemical structure that consists of two different molecular components, the hydrophilic group and the hydrophobic groups. A hydrophilic group is a water-soluble component, and a hydrophobic group is a water insoluble component. The soluble component, or hydrophilic group, is called the "head", and the hydrophobic group is called the "tail", as showed in Fig. 6.50. [30, 31]

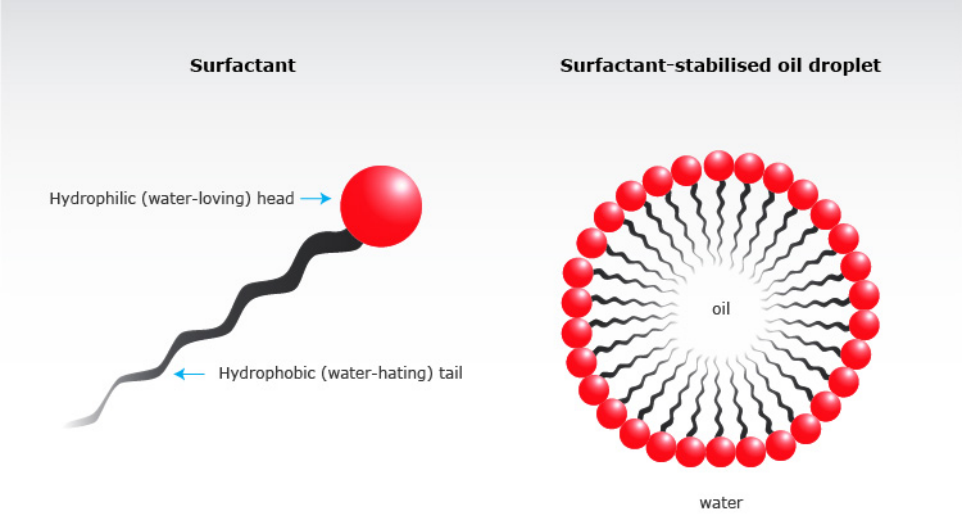

Figure 6.50: Surfactant. [8]

In Fig. 6.50 is possible to see the "head", the hydrophilic group and the "tail", the hydrophobic group.

The head and tail surfactants attack the interface between two immiscible surfaces, thus decreasing the

interfacial forces between the two surfaces.

Surfactants are frequently classified into four main categories, in accordance to the ionic nature of the head group, a surfactant can be anionic, cationic, nonionic or zwitterionic. Each type have certain characteristics depending on how the surfactant molecules ionize in aqueous solution. [31]

When a surfactant is injected the hydrophilic head interacts with water molecules and the hydrophobic tail interacts with the residual oil. By this, the surfactant can form water-in-oil or oil-in-water emulsions. Surfactant molecules are amphiphilic, since they have both hydrophilic and hydrophobic groups. [31]

A surfactant can be sensitive to high temperature and high salinity, therefore surfactants that can resist to these conditions should be used.

Thus, in this experiment a surfactant may be injected to reduce the IFT, and try to improve the oil recovery, making the oil move inside the core. Given the reservoir conditions, this surfactant should be resistant to high temperature and high salinity, and anionic.

Bibliography

[1] http://www.slb.com/services/technical_challenges/carbonates.aspx

[2] http://www.opusdei.org/en/article/going-to-mass-in-ruwais/

[3] https://www.sbc.slb.com/Our_Ideas/Energy_Perspectives/2nd%20Semester13_Content/2nd%20Semester%202013_Seizing.aspx

[4] Wael Abdallah, J.S.B., Carnegie, A.: Fundamentals of wettability. (2007)

[5] T. Puntervold, S.S., Austad, T.: Smart water as wettability modifier in carbonate and sandstone: A discussion of similarities/differences in the chemical mechanisms. (July 2009)

[6] Austad, T.: Water based eor in carbonates and sandstones: New chemical understanding of the eor-potential using “smart water”. (April 2012)

[7] http://www.corelab.com/cli/core-holders/standard-core-holder-hch-series

[8] http://sciencelearn.org.nz/Science-Stories/Where-Land-Meets-Sea/Sci-Media/Images/Surfactants

[9] Harbaugh, J.W.: Carbonate oil reservoir rocks. In: Stanford University, Stanford, Calif. (U.S.A.). Volume 5.

[10] Lutgens, F.K., Tarbuck, E.J.: Essentials of Geology. (2012)

[11] Tiab, D., Donaldson, E.C.: Petrophysics. (2004)

[12] Venezuela, M.: Report on eor methods. In: Report on EOR methods. (2008)

[13] J.J.Taber, F.M., Seright, R.: Eor screening criteria revisited - part 1: Introduction to screening criteria and enhanced recovery fields projects. (August 1997)

[14] Romero-Zeron, L.: Advances in enhanced oil recovery processes

[15] Pierre M. Lichaa, H.A., Abdul, J.H.: Wettability Evaluation of a Carbonate Reservoir Rock. (1992)

[16] Sharma, G., Mohanty, K.K.: Wettability alteration in high-temperature and high-salinity carbonate reservoirs. (August 2013)

[17] Morrowa, N.R., Mason, G.: Recovery of oil by spontaneous imbibition. (2001)

[18] L. Yu, S.E., Kleppe, H.: Spontaneous imbibition of seawater into preferentially oil-wet chalk cores — experiments and simulations. (February 2009)

[19] Hazim H. Al-Attar, M.Y.M., Ghannam, M.: Low-salinity flooding in a selected carbonate reservoir: experimental approach. (March 2013)

[20] M.B. Alotaibi, R.N., Nasr-El-Din, H.: Wettability challenges in carbonate reservoirs. (April 2010)

[21] S. Jafar Fathi, T.A., Strand, S.: Water-based enhanced oil recover (eor) by "smart water" in carbonate reservoirs. (April 2012)

[22] J. Romanuka, J.H., Austad, T.: Low salinity eor in carbonates. (April 2012)

[23] Adeel Zahid, E.H.S., Shapiro, A.A.: Smart waterflooding (high sal/low sal) in carbonate reservoirs. (June 2012)

[24] Zhang, Y., Sarma, H.: Improving waterflood recovery efficiency in carbonate reservoirs through salinity variations and ionic exchanges: A promising low-cost "smart-waterflood" approach. (November 2012)

[25] Loan T. Vo, R.G., Hehmeyer, O.J.: Ion chromatography analysis of advanced ion management carbonate coreflood experiments. (November 2012)

[26] David Levitt, A.K., Jouenne, S.: Overcoming design challenges of chemical eor in high-temperature, high salinity carbonates. (March 2013)

[27] H.H. Al-Attar, M.M., Zekri, A.: The impact of *LoSal* on oil recovery from a selected carbonate reservoir in abu dhabi-an experimental approach. (March 2013)

[28] Ali A. Yousef, S.A.S., Al-Jawfi, M.: Laboratory investigation of novel oil recovery method for carbonate reservoirs. (October 2010)

[29] Robin Gupta, T.W.W., Harris, C.R.: Enhanced waterflood for middle east carbonate cores - impact of injection water composition. (September 2011)

[30] ElMofty, O.: Surfactant enhanced oil recovery by wettability alteration in sandstone reservoirs. (Spring 2012)

[31] Sandersen, S.B.: Enhanced oil recovery with surfactant flooding. (May 2012)

Appendices

Appendix A

Ionic composition results for CC-01

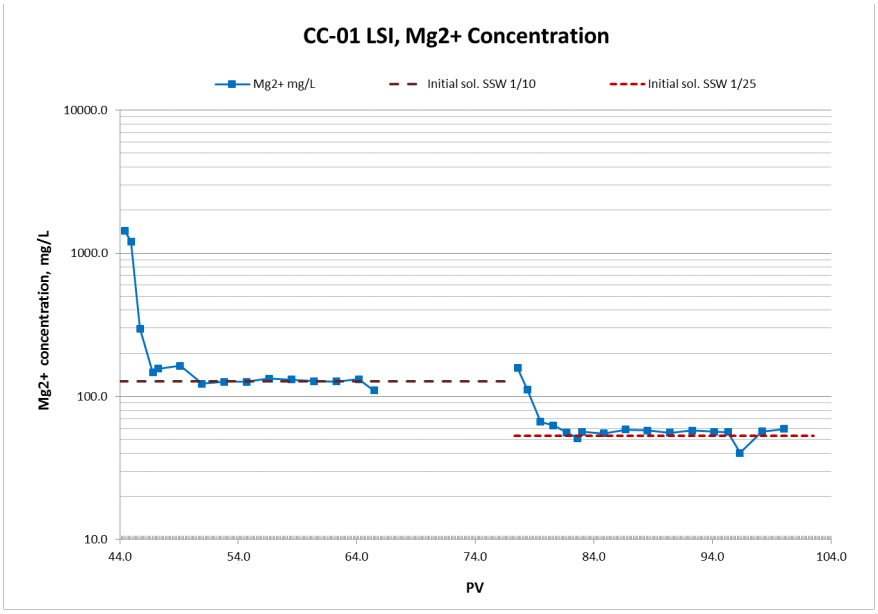

Figure A.51: Results of analyses performed to the effluent of core number 1 to measure the Magnesium concentration

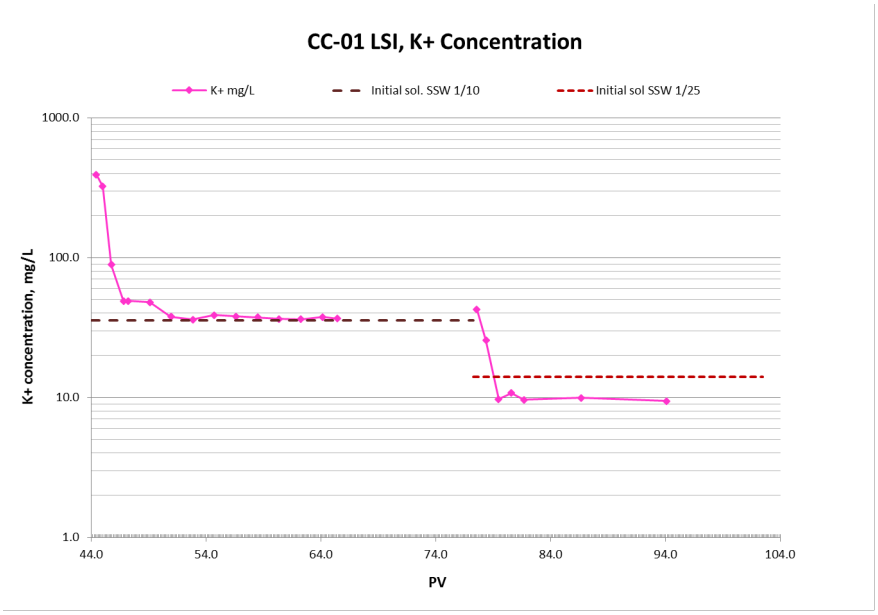

Figure A.52: Results of analyses performed to the effluent of core number 1 to measure the Potassium concentration

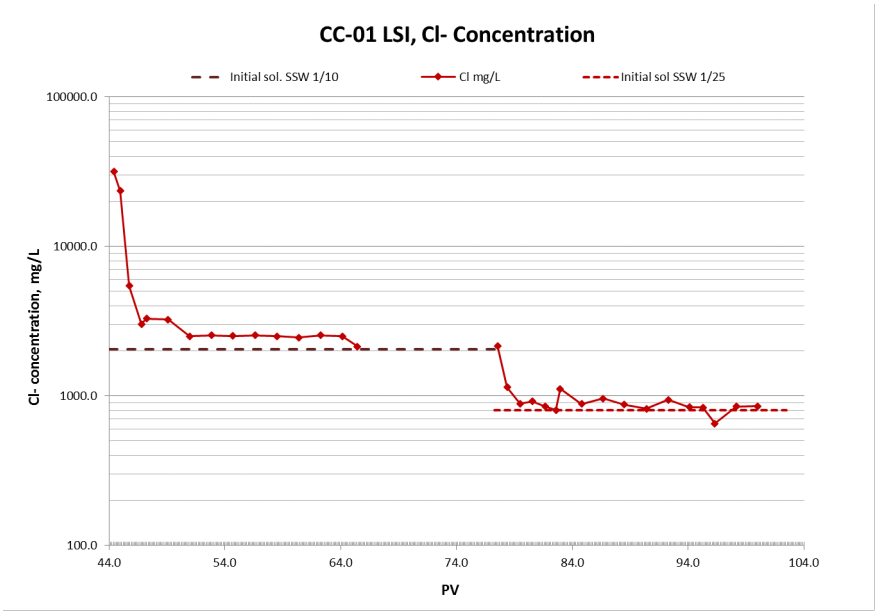

Figure A.53: Results of analyses performed to the effluent of core number 1 to measure the Chloride concentration

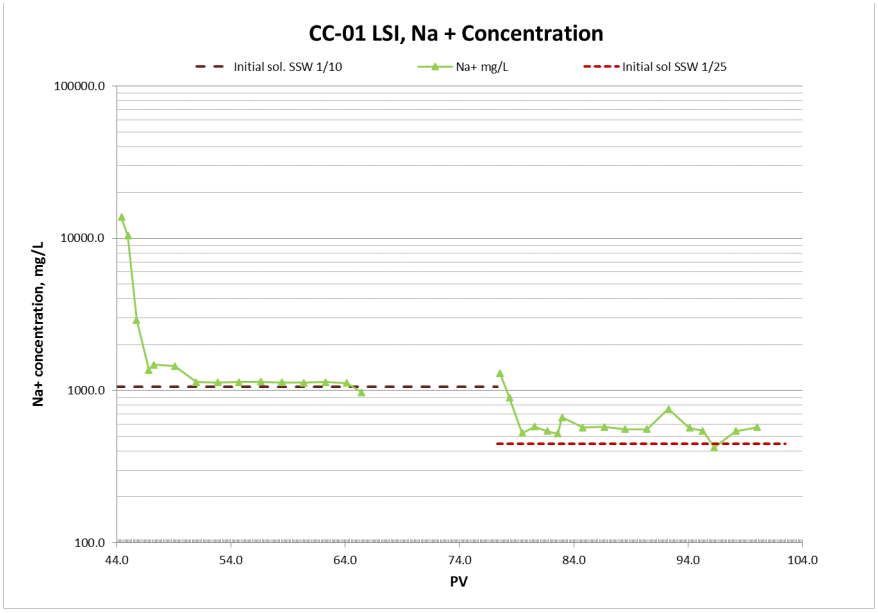

Figure A.54: Results of analyses performed to the effluent of core number 1 to measure the Sodium concentration

Appendix B

Ionic composition results for CC-02

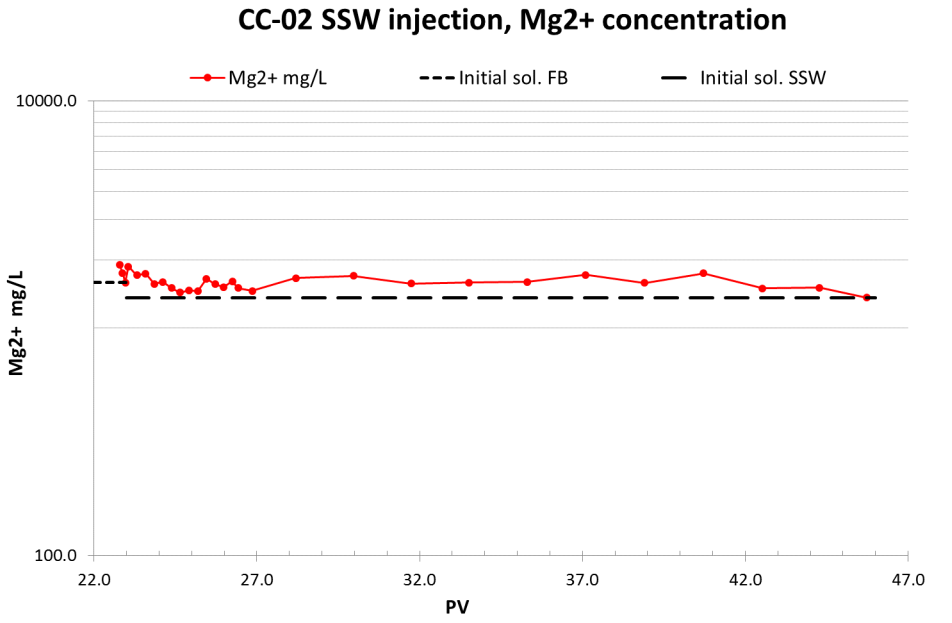

Figure B.55: Results of analyses performed to the effluent of SSW in core number 2 to measure the Magnesium concentration

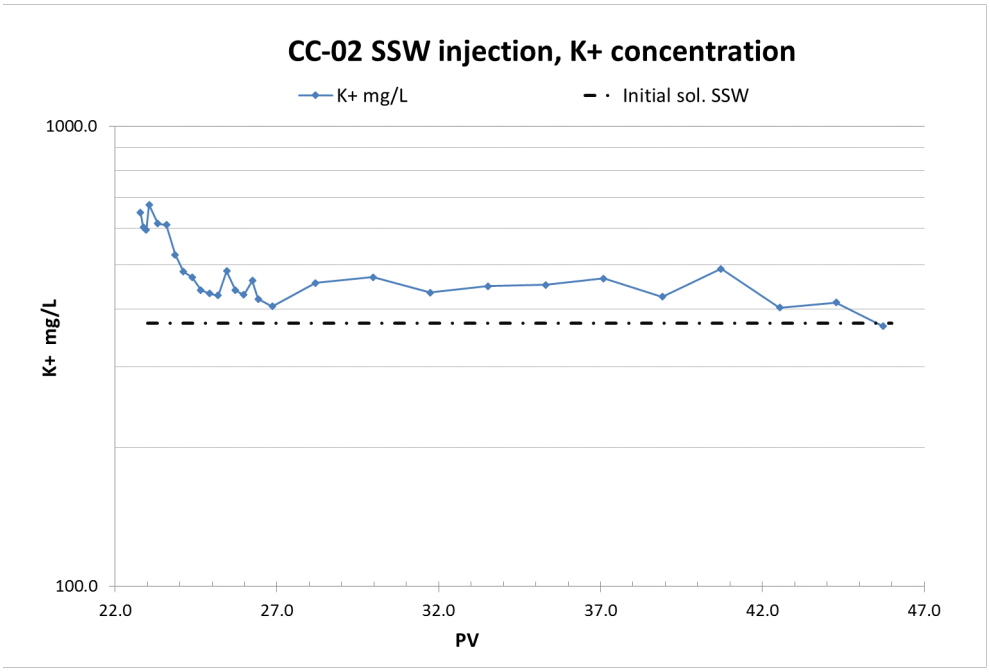

Figure B.56: Results of analyses performed to the effluent of SSW in core number 2 to measure the Potassium concentration

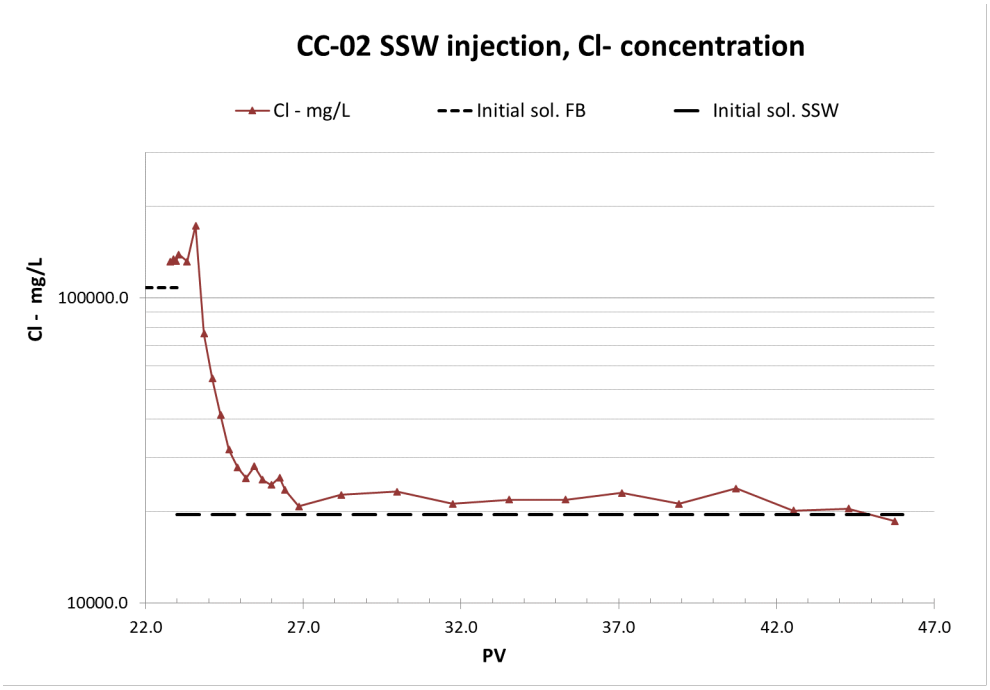

Figure B.57: Results of analyses performed to the effluent of SSW in core number 2 to measure the Chloride concentration

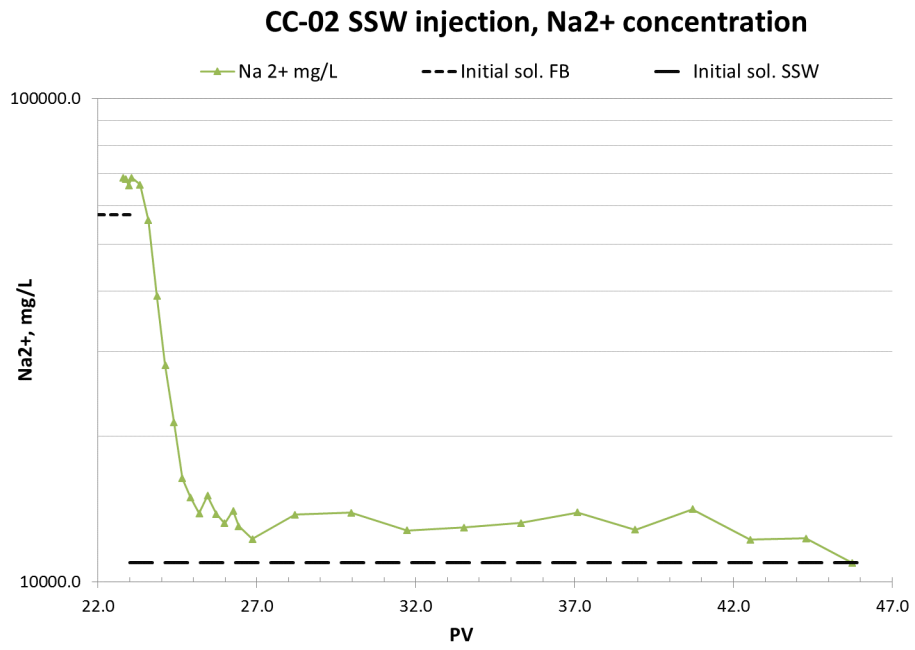

Figure B.58: Results of analyses performed to the effluent of SSW in core number 2 to measure the Sodium concentration

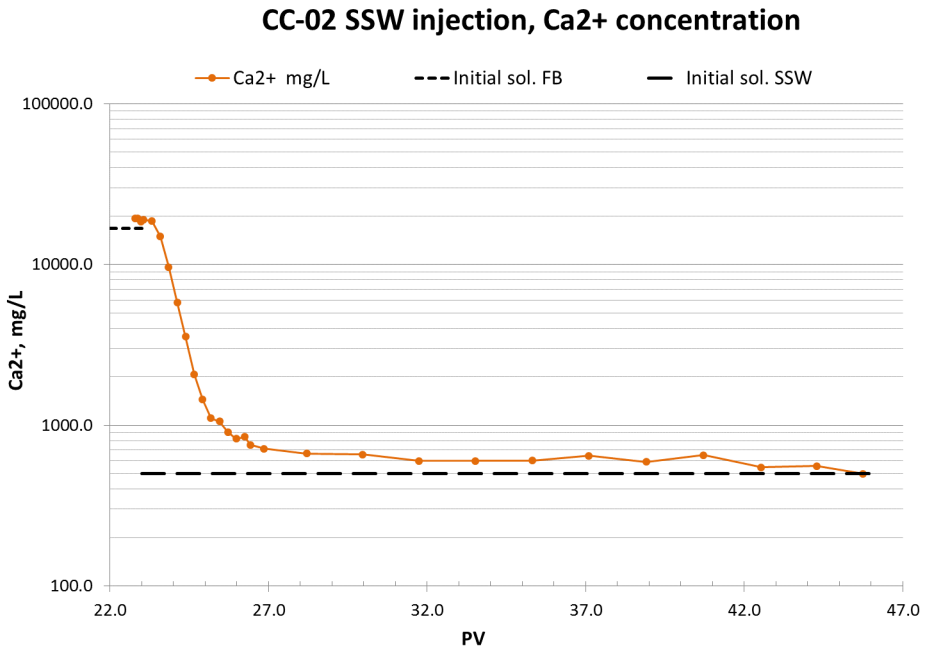

Figure B.59: Results of analyses performed to the effluent of SSW in core number 2 to measure the Calcium concentration

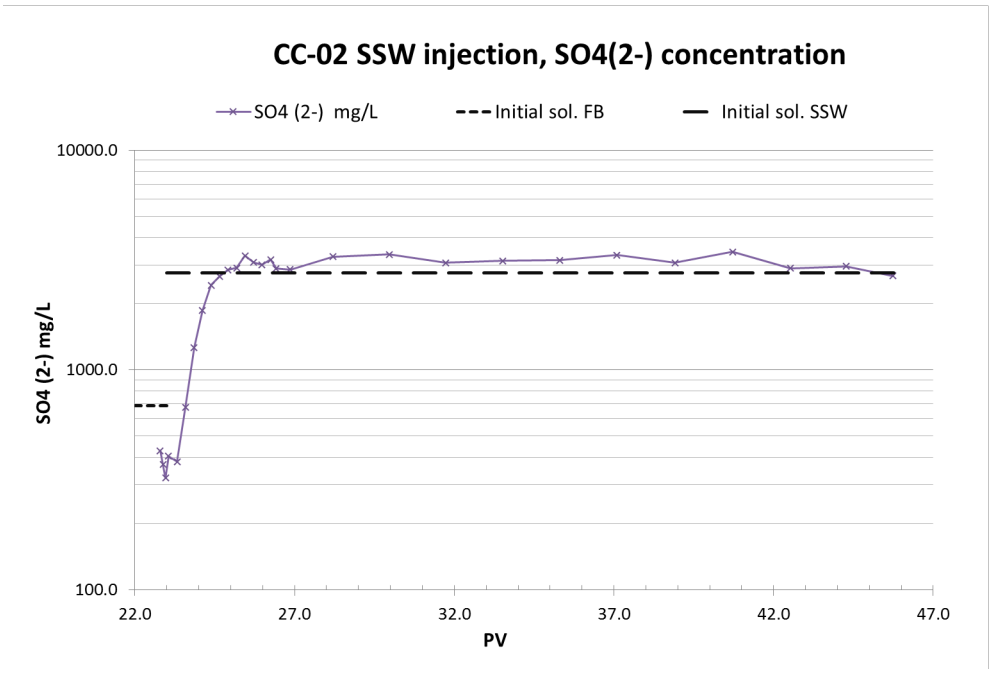

Figure B.60: Results of analyses performed to the effluent of SSW in core number 2 to measure the Sulphate concentration

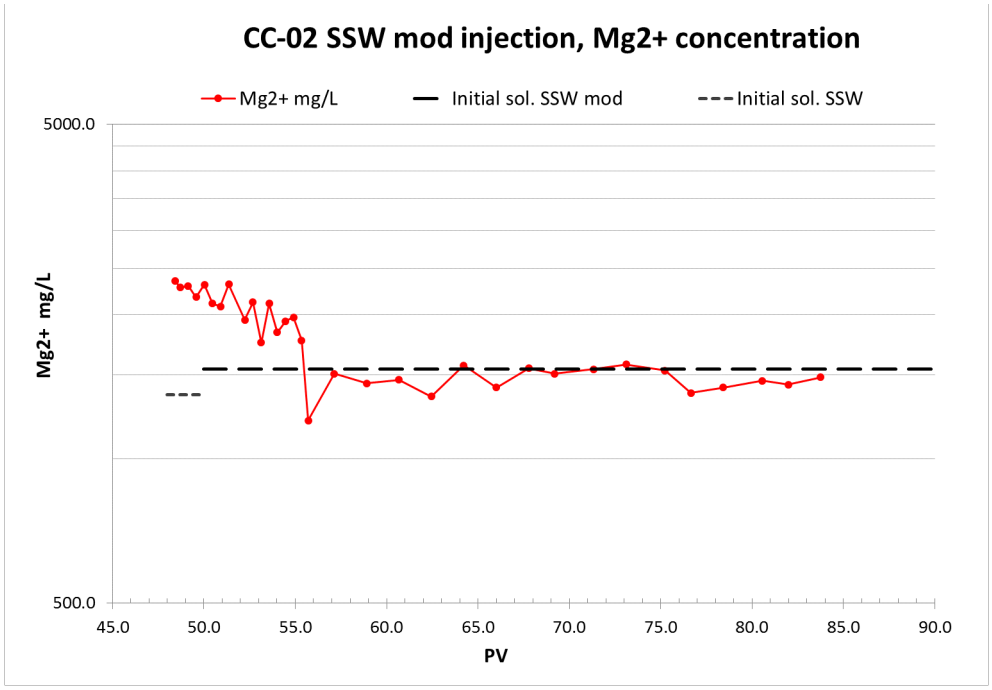

Figure B.61: Results of analyses performed to the effluent of SSW mod in core number 2 to measure the Magnesium concentration

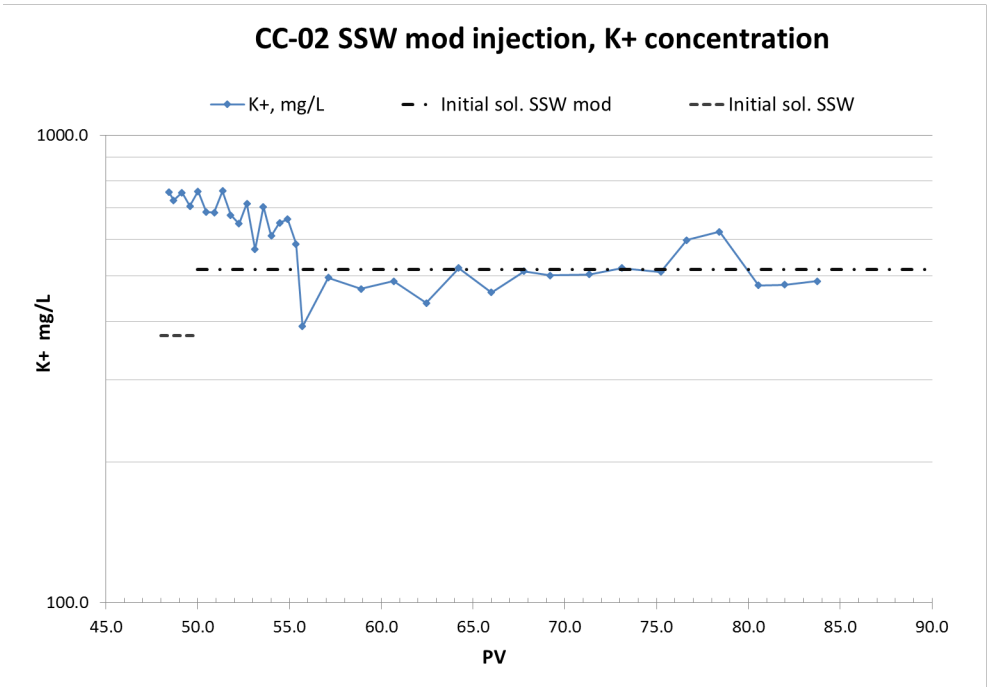

Figure B.62: Results of analyses performed to the effluent of SSW mod in core number 2 to measure the Potassium concentration

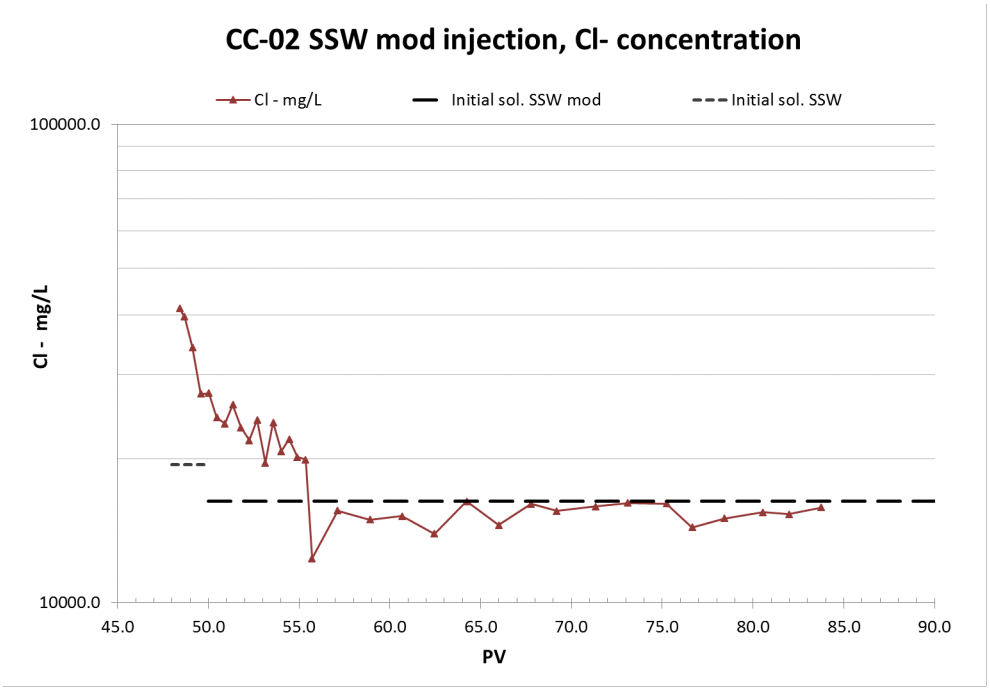

Figure B.63: Results of analyses performed to the effluent of SSW mod in core number 2 to measure the Chloride concentration

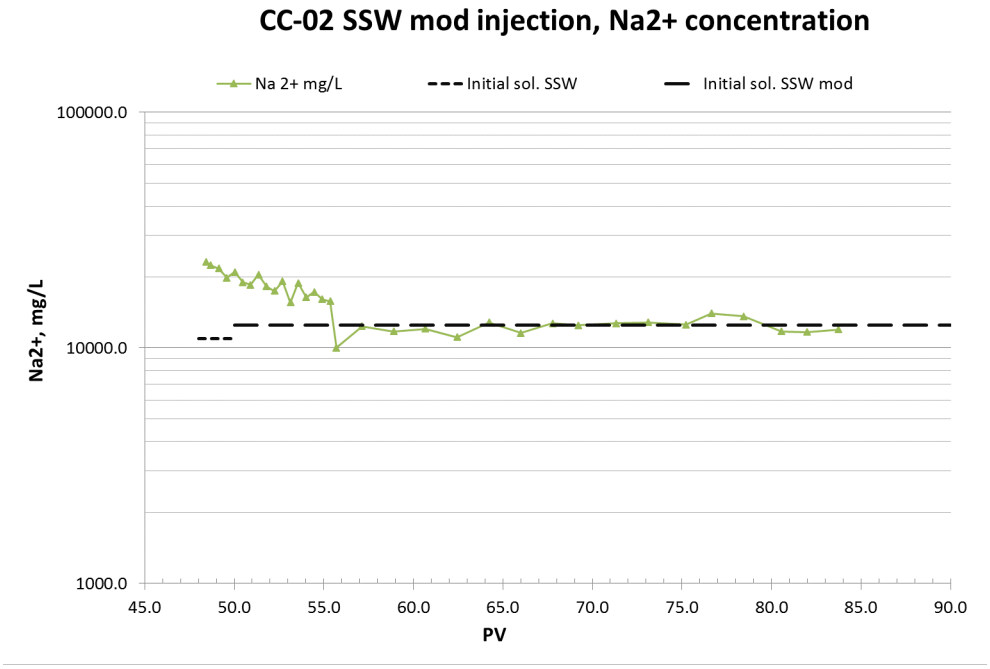

Figure B.64: Results of analyses performed to the effluent of SSW mod in core number 2 to measure the Sodium concentration

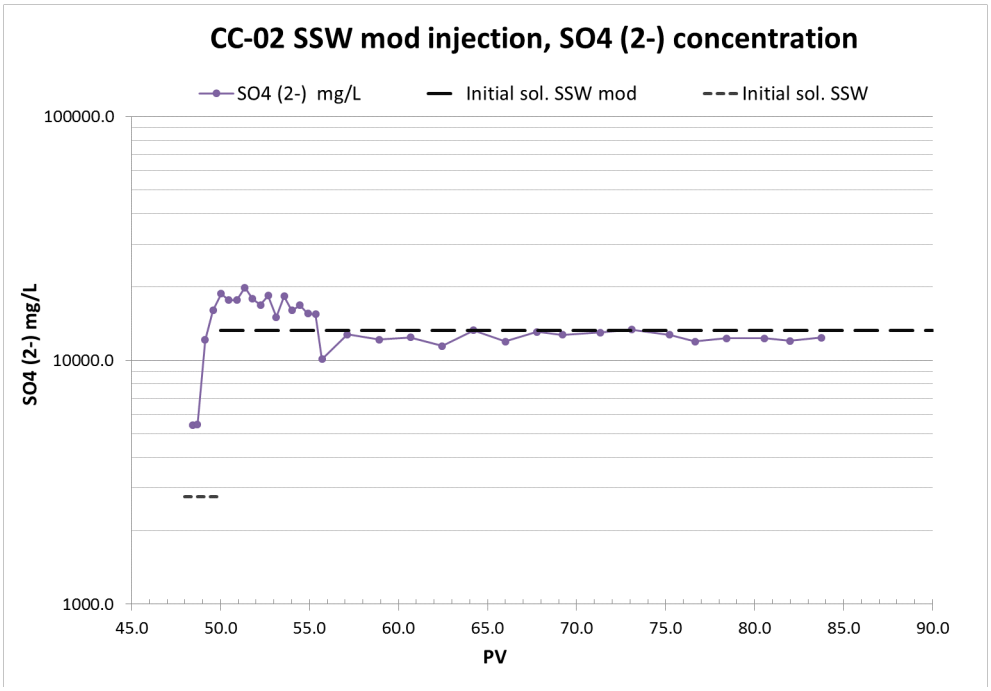

Figure B.65: Results of analyses performed to the effluent of SSW mod in core number 2 to measure the Sulphate concentration